Bulletin of Mathematical Biology (2019) 81:2396–2427
https://doi.org/10.1007/s11538-019-00611-2

Society for Mathematical Biology

Spatial Model for Oncolytic Virotherapy with Lytic Cycle Delay

Jiantao Zhao[1,2] · **Jianjun Paul Tian**[1,3]

Received: 13 December 2018 / Accepted: 7 May 2019 / Published online: 14 May 2019

Abstract

We formulate a mathematical model of functional partial differential equations for oncolytic virotherapy which incorporates virus diffusivity, tumor cell diffusion, and the viral lytic cycle based on a basic oncolytic virus dynamics model. We conduct a detailed analysis for the dynamics of the model and carry out numerical simulations to demonstrate our analytic results. Particularly, we establish the positive invariant domain for the ω limit set of the system and show that the model has three spatially homogenous equilibriums solutions. We prove that the spatially uniform virus-free steady state is globally asymptotically stable for any viral lytic period delay and diffusion coefficients of tumor cells and viruses when the viral burst size is smaller than a critical value. We obtain the conditions, for example the ratio of virus diffusion coefficient to that of tumor cells is greater than a value and the viral lytic cycle, is greater than a critical value, under which the spatially uniform positive steady state is locally asymptotically stable. We also obtain conditions under which the system undergoes Hopf bifurcations, and stable periodic solutions occur. We point out medical implications of our results which are difficult to obtain from models without combining diffusive properties of viruses and tumor cells with viral lytic cycles.

Keywords Oncolytic virotherapy · Functional reaction–diffusion equations · Stability · Hopf bifurcation

✉ Jianjun Paul Tian
jtain@nmsu.edu

[1] Department of Mathematical Sciences, New Mexico State University, Las Cruces, NM 88001, USA

[2] School of Mathematical Sciences, Heilongjiang University, Harbin 150080, Heilongjiang, People's Republic of China

[3] School of Mathematics and Computer Science, Shaanxi University of Technology, Hanzhong 723000, Shaanxi, People's Republic of China

1 Introduction

Oncolytic viruses are genetically altered viruses that can infect and multiply in cancer cells but leave healthy normal cells intact. Oncolytic viruses are of two types: oncolytic wild viruses that naturally occur preferentially in human cancer cells, and gene-modified viruses that are engineered to achieve selective oncolysis. Wild-type viruses have shown a limited oncolytic efficacy in some preclinical trials, while gene-modified viruses seem to have a great potency of oncolysis (Kirn and McCormick 1996; Kaplan 2005; Roberts et al. 2006). Before 1990s, case studies and small trials of various viruses in cancer therapy were reported (Chiocca 2002). Since 1990s, genetic engineering began to be used for oncolytic viruses (Martuza et al. 1991). So far, many types of viruses have been modified for experiments (Lawler et al. 2017), and some oncolytic viruses have been approved for human clinic trials (Maroun et al. 2017). However, the full potential of oncolytic viruses seem still not to have been reached (Chiocca and Rabkin 2014). One major challenge is how to make viruses spread thoroughly into solid tumors (Mok et al. 2009). Understanding of the spreading dynamics of oncolytic viruses through tumors can help to overcome this difficulty and possibly to develop strategies for clinical applications.

Mathematical modeling can allow us to explore the whole spectrum of possible outcomes and provide rationales to optimize treatments. Several attempts have been made to understand and characterize viral dynamics by mathematical models, see for example (Wu et al. 2001; Wodarz 2001; Bajzer et al. 2008; Friedman et al. 2006). These mathematical models can be divided into two classes roughly. One class uses ordinary differential equations (ODEs) including delay differential equations (DDEs) (Novozhilov et al. 2006; Karev et al. 2006; Wodarz and Komarova 2009; Tian 2011; Wang et al. 2013; Phan and Tian 2017; Vasiliu and Tian 2011; Boeuf et al. 1974; Choudhury and Nasipuri 2014; Wares et al. 2015; Barish et al. 2017; Mahasa et al. 2017; Jenner et al. 2018; Ratajczyk et al. 2018), and the other uses partial differential equations (PDEs) (Wu et al. 2001; Wein et al. 2003; Friedman et al. 2006; Wodarz et al. 2012; Wang et al. 2017; Timalsina et al. 2017; Friedman and Lai 2018). For PDE models of oncolytic virotherapy, most of them use ideas from fluid dynamics to model solid tumor growth where tumor cells convect in the fluid velocity field within the tumor and viruses simply diffuse within the tumor. All these modeling studies have provided certain insights to viral therapy. One study by Jain and colleagues particularly emphasizes the importance of the diffusive property of viruses (Mok et al. 2009). However, it is well known that the growth of solid tumors, particularly, brain tumor gliomas, also shows characters of cell diffusion (Harpold et al. 2007). It is, therefore, appropriate to combine diffusive tumor growth with virus diffusion into one mathematical model.

The viral lytic cycle is the time period of the intracellular viral life cycle starting from the time when a virus enters a cell to the time when a certain number (viral burst size) of newly replicated viruses come out upon the cell lysis. It is an important parameter of viral dynamics. The article (Wang et al. 2013) was the first to incorporate the viral lytic cycle as a delay parameter in a mathematical model for oncolytic viral therapy.

In this study, building on a basic mathematical model for oncolytic viral dynamics (Tian 2011; Wang et al. 2013), we combine the viral lytic cycle, tumor cell diffusion, and virus diffusion into a system of functional partial differential equations as a spatial

model for oncolytic viral therapy. Our spatial model considers a brain as a domain in $\mathbb{R}^3$ where a brain tumor grows and three populations, tumor cells, infected tumor cells, and intercellular-free viruses, interact with each other. We conduct a detailed analysis and computational demonstrations.

Although our analysis focuses on long-term (asymptotical) dynamical behaviors, we also obtain short-term information about virus and cell distributions which may also give insights to experiments and treatments. Comparing with non-spatial and non-delay models, our model reveals more relevant details of viral therapy. For example, when the ratio of diffusion coefficients between viruses and tumor cells is greater than a particular value, the spatially homogeneous equilibrium solution is stable for any length of the viral lytic cycle. A possible medical implication is that if we can genetically make oncolytic viruses diffuse faster than tumor cell diffuse, the time period of the viral lytic cycle will not affect the stabilization of treatments and may improve overall efficacy of treatments. This mathematical result does not contradict the fact that there is a functional relation between the viral lytic cycle and burst size which reveals that at a critical lytic cycle time, Hopf bifurcations occur in the model system (Tian 2011; Wang et al. 2013). In fact, for our spatial model, we also obtain a similar functional relation of bifurcation diagram for different ranges of parameter values. In addition, the diffusion coefficients of viruses and tumor cells with viral lytic cycle length have a combined effect on dramatic changes of the solutions, for example the occurrence of Hopf bifurcations and occurrence of stable periodic solutions. This theoretical result may explain various outcomes of oncolytic viral therapies in the current experimental research. Therefore, combining diffusive property of viruses and tumor cells with viral lytic cycle into one mathematical model is necessary to further our understanding for oncolytic viral therapy.

The rest of the paper is organized as follows. In Sect. 2, we review some basic mathematical models for oncolytic viral therapy and introduce our model in terms of delay reaction–diffusion equations. In Sect. 3, we mathematically analyze the dynamics of our functional PDE model for a solid tumor in $\mathbb{R}^3$. In Sect. 4, we demonstrate some numerical simulations in a two-dimensional spatial domain to support the theoretical results. In Sect. 5, we highlight our results which cannot be obtained without virus and cell diffusion, explain some medical implications of our results, and discuss and compare several relevant results in the literature. In "Appendix", we carry out analysis for properties of periodic solutions arising from Hopf bifurcations of functional partial differential equations which provides some guidance for numerical simulations and also briefly describe numerical methods we use to solve our model.

2 Mathematical Model

In the paper (Tian 2011), a basic mathematical model for oncolytic virotherapy was proposed as follows:

$$\begin{cases} \frac{\mathrm{d}u(t)}{\mathrm{d}t} = \alpha u(t)\left(1 - \frac{u(t)+w(t)}{K}\right) - \beta u(t)v(t), \\ \frac{\mathrm{d}w(t)}{\mathrm{d}t} = \beta u(t)v(t) - \delta w(t), \\ \frac{\mathrm{d}v(t)}{\mathrm{d}t} = b\delta w(t) - \beta u(t)v(t) - \gamma v(t). \end{cases} \tag{1}$$

Here, $u(t)$ stands for the uninfected tumor cell population at time t, $w(t)$ stands for the infected tumor cell population, and $v(t)$ stands for the free virus population. Tumor growth is modeled by logistic growth, and K is the maximum tumor population. The coefficient β represents infectivity of the virus. The infected tumor cells die with a rate δw. The parameter b is the burst size of the virus, the parameter γv is the clearance rate of free virus particles by various mechanisms including non-specific binding and generation of the defective interfering particles.

Viruses need time to complete their life cycle within cells. Incorporating the viral lytic cycle within infected tumor cells, in Wang et al. (2013), the following delay differential equation model was proposed.

$$\begin{cases} \frac{\mathrm{d}u(t)}{\mathrm{d}t} = \alpha u(t)\left(1 - \frac{u(t)+w(t)}{K}\right) - \beta u(t)v(t), \\ \frac{\mathrm{d}w(t)}{\mathrm{d}t} = \beta u(t-\tau)v(t-\tau) - \delta w(t), \\ \frac{\mathrm{d}v(t)}{\mathrm{d}t} = b\delta w(t) - \beta u(t)v(t) - \gamma v(t), \end{cases} \tag{2}$$

where τ stands for the mean time period of the viral lytic cycle.

Now, we assume that tumor cells diffuse with diffusion coefficient D_1, and viruses diffuse with diffusion coefficient D_2. It is an assumption to consider cell movement to only be by diffusion (Swanson et al. 2002; Massey et al. 2018). Based on the above mathematical models , we propose a spatial mathematical model for oncolytic viral therapy as follows:

$$\begin{cases} \frac{\partial u(x,t)}{\partial t} = D_1\Delta u(x,t) + \alpha u(x,t)\left(1 - \frac{u(x,t)+w(x,t)}{K}\right) - \beta u(x,t)v(x,t), \\ \frac{\partial w(x,t)}{\partial t} = D_1\Delta w(x,t) + \beta u(x,t-\tau)v(x,t-\tau) - \delta w(x,t), \\ \frac{\partial v(x,t)}{\partial t} = D_2\Delta v(x,t) + b\delta w(x,t) - \beta u(x,t)v(x,t) - \gamma v(x,t), \end{cases} \tag{3}$$

for which $x \in \Omega,\ t > 0$, where Ω is the brain tissue which is a domain in $\mathbb{R}^3$. To complete the model, we give the no-flux boundary conditions and initial conditions as follows:

$$\begin{cases} \frac{\partial u(x,t)}{\partial \mathbf{n}} = \frac{\partial w(x,t)}{\partial \mathbf{n}} = \frac{\partial v(x,t)}{\partial \mathbf{n}} = 0, \quad x \in \partial\Omega,\ t \geq 0; \\ u(x,t) = u_0(x,t) \geq 0,\ w(x,t) = w_0(x,t) \geq 0, \quad \text{and} \\ v(x,t) = v_0(x,t) \geq 0, \quad x \in \overline{\Omega}, \quad -\tau \leq t \leq 0. \end{cases} \tag{4}$$

In the boundary and initial conditions, $\partial\Omega$ stands for the brain tissue boundary, $\mathbf{n}$ stands for its normal direction, $\overline{\Omega}$ stands for the brain tissue with it boundary, and $u_0(x,t)$, $w_0(x,t)$, $v_0(x,t)$ are initial densities. The zero-flux boundary condition means that there are no tumor cells or viruses crossing the brain tissue boundary. The zero-flux boundary condition for tumor cells has biological significance and has been applied in many diffusion-type modeling of brain tumors (Swanson et al. 2002; Massey et al.

2018). This is also biologically meaningful for viruses since oncolytic viruses do not infect normal cells by definition which are confined within the tumor (Chiocca 2002).

We non-dimensionalize the system (3)–(4) by setting

$$\begin{aligned} &\bar{t} = \delta t,\ \bar{\tau} = \delta\tau,\ u(x,t) = K\bar{u}(x,\bar{t}),\ w(x,t) = K\bar{w}(x,\bar{t}),\ v(x,t) = K\bar{v}(x,\bar{t}),\\ &r = \frac{\alpha}{\delta},\ a = \frac{\beta K}{\delta},\ c = \frac{\gamma}{\delta},\ d_1 = \frac{D_1}{\delta},\ d_2 = \frac{D_2}{\delta},\\ &u_0(x,t) = K\bar{u}_0(x,\bar{t}),\ w_0(x,t) = K\bar{w}_0(x,\bar{t}),\ v_0(x,t) = K\bar{v}_0(x,\bar{t}). \end{aligned}$$

For convenience, dropping all bars over the variables, we have

$$\begin{cases} \frac{\partial u(x,t)}{\partial t} = d_1\Delta u(x,t) + ru(x,t)(1-u(x,t)-w(x,t)) - au(x,t)v(x,t),\\ \frac{\partial w(x,t)}{\partial t} = d_1\Delta w(x,t) + au(x,t-\tau)v(x,t-\tau) - w(x,t),\\ \frac{\partial v(x,t)}{\partial t} = d_2\Delta v(x,t) + bw(x,t) - au(x,t)v(x,t) - cv(x,t),\quad x\in\Omega,\ t>0;\\ \frac{\partial u(x,t)}{\partial \mathbf{n}} = \frac{\partial w(x,t)}{\partial \mathbf{n}} = \frac{\partial v(x,t)}{\partial \mathbf{n}} = 0,\quad x\in\partial\Omega,\ t\geq 0;\\ u(x,t) = u_0(x,t)\geq 0,\ w(x,t) = w_0(x,t)\geq 0,\quad \text{and}\\ v(x,t) = v_0(x,t)\geq 0,\quad x\in\overline{\Omega},\quad -\tau\leq t\leq 0. \end{cases} \tag{5}$$

3 Analysis of the Model

In this section, we study the properties of spatial homogenous equilibrium solutions and periodic solutions arising from Hopf bifurcations. The system (5) always has two spatially uniform steady states $E_0 = (0,0,0)$ and $E_1 = (1,0,0)$. When $b > b_0 = 1 + \frac{c}{a}$, the system (5) has three spatially uniform steady states E_0, E_1 and $E^* = (u^*, w^*, v^*)$, where

$$u^* = \frac{c}{a(b-1)},\ w^* = \frac{rc(ab-a-c)}{a(b-1)(rc+ab-a)},\ v^* = \frac{r(ab-a-c)}{a(rc+ab-a)}.$$

In Sect. 3.1, we establish positive invariant region as a sub-functional space for the ω limit sets of our model and prove that the spatially uniform steady state E_1 is globally asymptotically stable for any viral lytic period $\tau \geq 0$ when the viral burst size $b < b_0$. In Sect. 3.2, we obtain the conditions; for example, the ratio of diffusion coefficients $\frac{d_2}{d_1}$ is greater than some value, and the viral lytic cycle is greater than a critical value, under which the spatially uniform positive steady state is locally asymptotically stable. We also obtain some conditions under which the system undergoes Hopf bifurcations, and stable periodic solutions occur.

In what follows, we choose Ω be a open set in $\mathbb{R}^3$ and define the real-valued Sobolev space

$$X = \left\{ (u_1,u_2,u_3)^{\mathrm{T}} \in (W^{2,2}(\Omega))^3 : \frac{\partial u_1}{\partial \mathbf{n}} = \frac{\partial u_2}{\partial \mathbf{n}} = \frac{\partial u_3}{\partial \mathbf{n}} = 0, \text{ at } x\in\partial\Omega \right\}.$$

3.1 Stability of the Steady State of E_1

To simplify notations, we denote $u_1(t) = u(x,t),\ u_2(t) = w(x,t),\ u_3(t) = v(x,t)$ and $U(t) = (u_1(t), u_2(t), u_3(t))^T$. Then, the system (5) can be rewritten as an abstract differential equation in the phase space $\mathscr{C} = C([-\tau,\ 0],\ X)$,

$$\dot{U}(t) = D\Delta U(t) + G(U_t) \tag{6}$$

where $U_t(\cdot) = U(t+\cdot)$, $D = \mathrm{diag}(d_1, d_1, d_2)$ and $G : \mathscr{C} \to X$ are defined by

$$G(U_t) = \begin{pmatrix} ru_1(t)(1-u_1(t)-u_2(t)) - au_1(t)u_3(t) \\ au_1(t-\tau)u_3(t-\tau) - u_2(t) \\ bu_2(t) - au_1(t)u_3(t) - cu_3(t) \end{pmatrix}.$$

Let N be a operator satisfies

$$N(\varphi_t)(x) = \frac{\partial \varphi(x,t)}{\partial t} - D\Delta\varphi(x,t) - G(\varphi_t)(x),$$

where $\varphi_t(\theta)(x) = \varphi(x, t+\theta) = (\varphi_1(x,t+\theta), \varphi_2(x,t+\theta), \varphi_3(x,t+\theta))$. Then, $N(0,0,0) = 0 \le 0 = N(u_t, w_t, v_t)(x)$, where $u_t(\theta)(x) = u(x,t+\theta),\ w_t(\theta)(x) = w(x,t+\theta),\ v_t(\theta)(x) = v(x,t+\theta)$. Noticing the homogeneous Neumann boundary and nonnegative initial value of system (5), we get $(0,0,0)$ is a lower solution of system (5), and by the comparison principle we know that the solution (u, w, v) of system (5) satisfies $u(x,t) \ge 0,\ w(x,t) \ge 0,\ v(x,t) \ge 0$ for $t \ge 0$.

From the nonnegativity of the solution, we have

$$\frac{\partial u}{\partial t} \le d_1\Delta u + ru(1-u).$$

The standard comparison theorem for parabolic boundary value problems implies that $u(x,t) \le U_1(z,t)$ in $\overline{\Omega} \times [0,\infty]$, where $U_1(x,t)$ is the positive solution of

$$\begin{cases} \dfrac{\partial U_1}{\partial t} = d_1\Delta U_1 + rU_1(1-U_1), & x \in \Omega,\ t > 0, \\ \dfrac{\partial U_1}{\partial \mathbf{n}} = 0, & x \in \partial\Omega,\ t > 0, \\ U_1(x,0) = u_0(x,0) > 0, & x \in \overline{\Omega}. \end{cases}$$

It is well known that $U_1(x,t) \to 1$ as $t \to \infty$. So we have $\limsup_{t\to\infty} u(x,t) \le 1$. For any $\varepsilon > 0$, there exists a $T_1 > 0$ such that $u(x,t) \le 1+\varepsilon$ in $\overline{\Omega} \times (T_1, \infty)$. When $t > T_1$, we have

$$\begin{aligned}
&\frac{\partial(u(x,t-\tau)+w(x,t))}{\partial t}\\
&= d_1\Delta(u(x,t-\tau)+w(x,t))\\
&\quad + ru(x,t-\tau)(1-u(x,t-\tau)-w(x,t-\tau))-w(x,t)\\
&\le d_1\Delta(u(x,t-\tau)+w(x,t))+r(1+\varepsilon)(1-u(x,t-\tau))-w(x,t)\\
&\le d_1\Delta(u(x,t-\tau)+w(x,t))+r(1+\varepsilon)-r_1(u(x,t-\tau)+w(x,t))
\end{aligned}$$

where $r_1 = \min\{1, r\}$. Similar to the previous discussion and noticed the sufficiently small properties of ε, we get $\limsup_{t\to\infty}(u(x,t-\tau), w(x,t)) \le \frac{r}{r_1}$. Since $u(x,t-\tau) \ge 0$, we have $\limsup_{t\to\infty} w(x,t) \le \frac{r}{r_1}$. There exists a $T_2 > T_1 + \tau$ such that $w(x,t) \le \frac{r}{r_1} + \varepsilon$ in $\overline{\Omega}\times(T_2,\infty)$. Then, from the third equation of (5)

$$\frac{\partial v(x,t)}{\partial t} \le d_2\Delta v + bw(x,t) - cv(x,t) \le d_2\Delta v + b\left(\frac{r}{r_1}+\varepsilon\right) - cv(x,t),\ t > T_2.$$

Similar to the previous discussion, we get $\limsup_{t\to\infty} \le \frac{br}{cr_1}$.

We define $\mathcal{C}^+ = C(\overline{\Omega}\times[-\tau,0],\mathbb{R}^+)$ with norm $||\varphi_t|| = \sup_{(x,\theta)\in\overline{\Omega}\times[-\tau,0]}\varphi(x,t+\theta)$. From the previous discussion, we have the following result.

Lemma 3.1 *The solution of the system* (5) *is ultimately uniformly bounded in* $\mathcal{C}^+ \times \mathcal{C}^+ \times \mathcal{C}^+$.

The ω limit set of the system (5) is contained in the bounded region:

$$R = \left\{(u_t, w_t, v_t) \in \mathcal{C}^+\times\mathcal{C}^+\times\mathcal{C}^+ : ||u_t|| \le 1, ||w_t|| \le \frac{r}{r_1}, ||v_t|| \le \frac{br}{cr_1}\right\}.$$

It is easy to verify that the region R is positively invariant for the system (5). In the rest of this paper, we will discuss the system (5) in region R.

From the above discussion, $(\bar{u}, \bar{w}, \bar{v})$ is a upper solution when the initial value is in the domain R , where $\bar{u}, \bar{w}, \bar{v}$ is the solution of the following system, respectively,

$$\begin{cases}
\frac{\partial\bar{u}(x,t)}{\partial t} = d_1\Delta\bar{u}(x,t) + r\bar{u}(x,t)(1-\bar{u}(x,t)), & x\in\Omega,\ t>0;\\
\frac{\partial\bar{u}(x,t)}{\partial\nu} = 0, & x\in\partial\Omega,\ t\ge 0;\\
\bar{u}(x,t) = u_0(x,t)\ge 0, & x\in\overline{\Omega},\ -\tau\le t\le 0,
\end{cases}$$

$$\begin{cases}
\frac{\partial\bar{w}(x,t)}{\partial t} = d_1\Delta\bar{w}(x,t) + \frac{abr}{cr_1} - \bar{w}(x,t), & x\in\Omega,\ t>0;\\
\frac{\partial\bar{w}(x,t)}{\partial\nu} = 0, & x\in\partial\Omega,\ t\ge 0;\\
\bar{w}(x,t) = w_0(x,t)\ge 0, & x\in\overline{\Omega},\ -\tau\le t\le 0,
\end{cases}$$

$$\begin{cases}
\frac{\partial\bar{v}(x,t)}{\partial t} = d_2\Delta\bar{v}(x,t) + \frac{br}{r_1} - c\bar{v}(x,t), & x\in\Omega,\ t>0;\\
\frac{\partial\bar{v}(x,t)}{\partial\nu} = 0, & x\in\partial\Omega,\ t\ge 0;\\
\bar{v}(x,t) = v_0(x,t)\ge 0, & x\in\overline{\Omega},\ -\tau\le t\le 0.
\end{cases}$$

Furthermore, $G(\varphi)$ satisfies a Lipschitz condition; therefore, the system (5) has a unique classical solution when initial value is in the domain R.

Linearizing system (6) at E_1, we have

$$\dot{U}(t) = D\Delta U(t) + L_{E_1}(U_t), \tag{7}$$

where

$$L_{E_1}(U_t) = \begin{pmatrix} -r & -r & -a \\ 0 & -1 & 0 \\ 0 & b & -a-c \end{pmatrix} \begin{pmatrix} u_1(t) \\ u_2(t) \\ u_3(t) \end{pmatrix} + \begin{pmatrix} 0\,0\,0 \\ 0\,0\,a \\ 0\,0\,0 \end{pmatrix} \begin{pmatrix} u_1(t-\tau) \\ u_2(t-\tau) \\ u_3(t-\tau) \end{pmatrix}.$$

From Wu (2012), the corresponding integral equation of (6) is

$$U(t) = T(t)U(0) + \int_0^t T(t-s)L_{E_1}(U_s)\mathrm{d}s, \tag{8}$$

where $T(t)$ is a C_0 semigroup generated by $D\Delta$. And its characteristic equation is given by

$$\lambda y - D\Delta y - L_{E_1}(e^{\lambda \cdot} y) = 0, \tag{9}$$

where $y \in \mathrm{dom}(\Delta)\backslash\{0\}$, $\mathrm{dom}(\Delta) \subset X$ and $e^{\lambda \cdot}(\theta)y = e^{\lambda\theta}y$, for $\theta \in [-\tau, 0]$. It is known that the eigenvalue problem

$$\begin{cases} -\Delta\phi = \mu\phi, & x \in \Omega, \\ \frac{\partial\phi}{\partial \mathbf{n}} = 0, & x \in \partial\Omega, \end{cases}$$

has eigenvalues μ_n, $n \in \mathbb{N}_0 = \mathbb{N}\cup\{0\}$, with corresponding eigenfunctions $\phi_n(x)$, and μ_n satisfy $0 = \mu_0 < \mu_1 \le \mu_2 \le \cdots \le \mu_n \le \cdots$. By using the Fourier expansion in (9),

$$y = \sum_{n=0}^{\infty} \begin{pmatrix} a_n \\ b_n \\ c_n \end{pmatrix} \phi_n(x),$$

where $a_n, b_n, c_n \in \mathbb{C}$, we know that the characteristic Eq. (9) is equivalent to

$$\det \begin{pmatrix} \lambda + d_1\mu_n + r & r & a \\ 0 & \lambda + d_1\mu_n + 1 & -a\mathrm{e}^{-\lambda\tau} \\ 0 & -b & \lambda + d_2\mu_n + a + c \end{pmatrix} = 0, \quad n \in \mathbb{N}_0.$$

That is, each eigenvalue λ is a root of the equation

$$(\lambda + d_1\mu_n + r)(\lambda^2 + T_n\lambda + D_n - ab\mathrm{e}^{-\lambda\tau}) = 0, \quad n \in \mathbb{N}_0, \tag{10}$$

where $T_n = (d_1 + d_2)\mu_n + a + c + 1$, $D_n = d_1d_2\mu_n^2 + [d_1(a+c) + d_2]\mu_n + a + c$. By discussing the distribution of the roots of (10), we have the following Lemma.

Lemma 3.2 *E_1 is locally asymptotically stable when $b < 1 + \frac{c}{a}$. E_1 is unstable when $b > 1 + \frac{c}{a}$.*

Proof Obviously, $\lambda_{1,n} = -d_1\mu_n - r < 0,\ n \in \mathbb{N}_0$ are roots of (10). We only need to discuss the roots of

$$\lambda^2 + T_n\lambda + D_n - abe^{-\lambda\tau} = 0,\ n \in \mathbb{N}_0. \tag{11}$$

When $\tau = 0$, noticed that $T_n^2 - 4(D_n - ab) = (d_1 - d_2)^2\mu_n^2 + 2(a + c + 1)(d_1 + d_2)\mu_n + (a + c - 1)^2 + 4ab > 0$, we get Eq. (11) which has two series real roots

$$\lambda_{2,n} = -\frac{1}{2}T_n - \frac{1}{2}\sqrt{T_n^2 - 4(D_n - ab)},\ n \in \mathbb{N}_0,$$
$$\lambda_{3,n} = -\frac{1}{2}T_n + \frac{1}{2}\sqrt{T_n^2 - 4(D_n - ab)},\ n \in \mathbb{N}_0.$$

Clearly, $\lambda_{2,n} < 0$ for $n \in \mathbb{N}_0$. And $\lambda_{3,n} < 0$ for all $n \in \mathbb{N}_0$ if and only if $b < 1 + \frac{c}{a}$. We claimed that all the roots have negative real parts when $b < 1 + \frac{c}{a}$ and $\tau > 0$. Otherwise, we assume (11) have a pure imaginary root $\mathrm{i}\nu_n$ for some $\tau > 0$; then, we have

$$-\nu_n^2 + \mathrm{i}T_n\nu_n + D_n - ab(\cos\nu_n\tau - \mathrm{i}\sin\nu_n\tau) = 0.$$

Separating the real and imaginary parts gives

$$\begin{cases} -\nu_2 + D_n = ab\cos\nu_n\tau, \\ -T_n\nu_n = ab\sin\nu_n\tau. \end{cases}$$

Furthermore, we need

$$\nu_n^4 + (T_n^2 - 2D_n)\nu_n^2 + D_n^2 - a^2b^2 = 0. \tag{12}$$

Denote $Q_n(z) = z^2 + (T_n^2 - 2D_n)z + D_n^2 - a^2b^2$. Obviously,

$$T_n^2 - 2D_n = (d_1^2 + d_2^2)\mu_n^2 + [2d_1 + 2(a + c)d_2]\mu_n + (a + c)^2 + 1 > 0.$$

If $b < 1 + \frac{c}{a}$, then

$$D_n^2 - a^2b^2 = \left\{d_1d_2\mu_n^2 + [d_1(a + c) + d_2]\mu_n\right\}^2 + 2(a + c)\left\{d_1d_2\mu_n^2 + [d_1(a + c) + d_2]\mu_n\right\} + (a + c)^2 - a^2b^2 > 0.$$

So $Q_n(z)$ has no positive roots when $b < 1 + \frac{c}{a}$. We know that (12) is always not valid when $b < 1 + \frac{c}{a}$. This is a contradiction. □

Remark 3.3 The spatially uniform steady state E_0 of the system (5) is always unstable because there has an eigenvalue $r > 0$.

Theorem 3.4 *If $b < b_0 = 1 + \frac{c}{a}$, then the spatially uniform steady state E_1 of the system (5) is globally asymptotically stable for $\tau \geq 0$.*

Proof Define a Lyapunov functional on the region R by

$$V(\phi_t)(x) = \int_\Omega \left(b\varphi_t^2(x,0) + \varphi_t^3(x,0) + ba \int_{-\tau}^{0} \varphi_t^1(x,\theta)\varphi_t^3(x,\theta)\mathrm{d}\theta \right) \mathrm{d}x$$

where $\phi_t(\theta) = (\varphi_t^1(\theta), \varphi_t^2(\theta), \varphi_t^3(\theta))$, $\varphi_t^i(\theta)(x) = \varphi^i(x, t+\theta)$, $i = 1, 2, 3$. When $b < b_0$, by virtue of the Neumann boundary condition, we obtain that

$$\begin{aligned} \dot{V}(\phi_t) &= \textstyle\int_\Omega [a(b-1)\varphi_t^1(x,0) - c]\varphi_t^3(x,0)\mathrm{d}x \\ &\leq \textstyle\int_\Omega [a(b-1) - c]\varphi_t^3(x,0)\mathrm{d}x \leq 0. \end{aligned}$$

And $\dot{V}(\phi_t) = 0$ if and only if $\varphi_t^3(x,0) = 0$. Furthermore, we can get the maximum invariant set in $\{\phi \in R : \dot{V}(\phi_t) = 0\}$ is the single point set $\{E_1\}$. The Lasalles invariance principle implies that E_1 is globally attractive. By Lemma 3.2, we get E_1 is global asymptotically stable for $\tau \geq 0$. □

3.2 Stability of the Positive Steady State E^* and Hopf Bifurcations

If $b > b_0 = 1 + \frac{c}{a}$, the system (5) has a spatially uniform positive steady state E^*. In this subsection, we always assume that $b > b_0 = 1 + \frac{c}{a}$ holds.

Linearizing the system (5) at E^*, we get

$$\dot{U}(t) = D\Delta U(t) + L_{E^*}(U_t),$$

where

$$L_{E^*} = L_1\phi(0) + L_2\phi(-\tau)$$

with

$$L_1 = \begin{pmatrix} -ru^* & -ru^* & -au^* \\ 0 & -1 & 0 \\ -av^* & b & -au^* - c \end{pmatrix} \text{ and } L_2 = \begin{pmatrix} 0 & 0 & 0 \\ av^* & 0 & au^* \\ 0 & 0 & 0 \end{pmatrix},$$

for $\varphi(\theta) = (\varphi_1(\theta), \varphi_2(\theta), \varphi_3(\theta))^{\mathrm{T}}$. Similar to the previous subsection, we find that the characteristic equation is equivalent to

$$\lambda^3 + a_{2,n}\lambda^2 + a_{1,n}\lambda + a_{0,n} + (b_{1,n}\lambda + b_{0,n})\mathrm{e}^{-\lambda\tau} = 0, \quad n \in \mathbb{N}_0, \tag{13}$$

where

$$
\begin{aligned}
a_{2,n} &= (2d_1 + d_2)\mu_n + \frac{rc + abc + ab - a}{a(b-1)},\\
a_{1,n} &= (d_1^2 + 2d_1d_2)\mu_n^2 + \left[\frac{rc + 2abc + a^2b - a^2}{a(b-1)}d_1 + \frac{rc + ab - a}{a(b-1)d_2}\right]\mu_n\\
&\quad + \frac{rc(bc + b - 1)}{a(b-1)^2} + \frac{bc}{b-1} - \frac{rc(ab - a - c)}{(b-1)(rc + ab - a)},\\
a_{0,n} &= d_1^2d_2\mu_n^3 + \left[\frac{bc}{b-1}d_1^2 + \frac{rc + ab - a}{a(b-1)}d_1d_2\right]\mu_n^2\\
&\quad + \left[\left(\frac{bc(rc + ab - a)}{a(b-1)^2} - \frac{rc(ab - a - c)}{a(b-1)(rc + ab - a)}\right)d_1 + \frac{rc}{a(b-1)}d_2\right]\mu_n\\
&\quad + \frac{rbc^2}{a(b-1)^2} - \frac{rc(ab - a - c)}{(b-1)(rc + ab - a)},\\
b_{1,n} &= \frac{r^2c(ab - a - c)}{(b-1)(rc + ab - a)} - \frac{bc}{b-1},\\
b_{0,n} &= \left[\frac{r^2c(ab - a - c)}{a(b-1)(rc + ab - a)}d_2 - \frac{bc}{b-1}d_1\right]\mu_n\\
&\quad - \frac{rbc^2}{a(b-1)^2} + \frac{rc(ab - a - c)(ab + rc)}{a(b-1)(rc + ab - a)}.
\end{aligned}
$$

When $\tau = 0$, the characteristic Eq. (13) becomes the following sequence of equations

$$\lambda^3 + a_{2,n}\lambda^2 + (a_{1,n} + b_{1,n})\lambda + a_{0,n} + b_{0,n} = 0, \quad n \in \mathbb{N}_0. \tag{14}$$

By the Routh–Hurwitz Criterion, all roots of (14) have negative real parts if and only if

$$
\begin{aligned}
H_{1,n} = a_{2,n} > 0,\ H_{2,n} &= a_{2,n}(a_{1,n} + b_{1,n})\\
&\quad - a_{0,n} - b_{0,n} > 0,\ H_{3,n} = (a_{0,n} + b_{0,n})H_{2,n} > 0
\end{aligned}
$$

for $n \in \mathbb{N}_0$. When $b > b_0$, we can see that $a_{2,n} > 0$ and $a_{0,n} + b_{0,n} > 0$ for $n \in \mathbb{N}_0$. So when

$$(\mathcal{H})\ \ b > b_0,\ a_{2,n}(a_{1,n} + b_{1,n}) - a_{0,n} - b_{0,n} > 0,$$

all roots of (14) have negative real parts. We get the following conclusion.

Lemma 3.5 *If* $(\mathcal{H})$ *holds, the spatially uniform positive steady state* E^* *of the system* (5) *is locally asymptotically stable when* $\tau = 0$.

Now, we look for sufficient conditions to ensure $H_{2,n} > 0$. By calculation, we have

$$H_{2,n} = 2d_1(d_1 + d_2)^2\mu_n^3 + A_3\mu_n^2 + (A_1d_1 + A_2d_2)\mu_n + H_{2,0}$$

where

$$
\begin{aligned}
A_1 &= \frac{(rc+abc+ab-a)(a^2b-a^2+2abc+rc)}{a^2(b-1)^2} \\
&\quad + \frac{rc[2c(rc+ab)+(b-1)(3a+2ra-a^2)+c]}{a(b-1)(rc+ab-a)} - \frac{rc(b-2c)}{a(b-1)^2}, \\
A_2 &= \frac{(rc+abc+ab-a)(rc+ab-a)}{a^2(b-1)^2} + \frac{rbc^2}{a(b-1)^2} - \frac{rc(ab-a-c)}{a(b-1)(rc+ab-a)}, \\
A_3 &= \left[\frac{4abc+3rc}{a(b-1)} + 2a + 1\right] d_1^2 + \frac{rc+ab-a}{a(b-1)} d_2^2 \\
&\quad + \left[\frac{4rc+2ac+2abc}{a(b-1)} + 2c + a + 3\right] d_1 d_2, \\
H_{2,0} &= \frac{rc(rc+abc+ab-a)}{a^2(b-1)^2}\left[\frac{rc(bc+b-1)}{(b-1)} + \frac{(ab-a-c)(r-a)}{rc+ab-a}\right] \\
&\quad - \frac{rc(ab-a-c)}{a(b-1)}.
\end{aligned}
$$

If $b > b_0$, then $A_3 > 0$. We define a function $\psi(x)$ by

$$
\begin{aligned}
\psi(x) = &-a^3x^4 + [c^3 + 3c + r + 1 - (c-1)a^3]x^3 \\
&+ [(c^2 + 3c + r + 1)rca - 3(2c + r + 1)a^2 - (3 - 2c)a^3]x^2 \\
&+ [r^2c^3 - (3c + 2r + 2)rca - (c^2 - 3c - 3r - 3)a^2 - (c-1)a^3]x \\
&+ rc(r+1)a - (r+1)a^2.
\end{aligned}
$$

It is easy to see that

$$
H_{2,0} = \frac{rc\psi(b)}{a(b-1)^3(rc+ab-a)}.
$$

When $b > b_0$, $\operatorname{sign}\{H_{2,0}\} = \operatorname{sign}\{\psi(b)\}$. Since

$$
\psi(b_0) = c^3(r+1)\left[r + a + 2c + 2 + \frac{(c+1)(r+c+1)}{a}\right] > 0
$$

and $\psi(x) \to -\infty$ as $x \to \pm\infty$, so $\psi(x)$ has at least one root and at most three root greater than b_0. According to the distribution of the roots of $\psi(x)$, we have the following two cases:

Case I: $\psi(b)$ has only root $b_1 > b_0$ or has three roots b_1, b_2, b_3 which are greater than b_0. When it has three roots which greater than b_0, the three roots are satisfied $b_1 < b_2 = b_3$ or $b_1 = b_2 = b_3$.

Case II: $\psi(b)$ has three roots b_1, b_2, b_3 that are greater than b_0, and the three roots are satisfied $b_1 \le b_2 < b_3$.

When Case I occurs, if $b \in (b_0, b_1)$, then $H_{2,0} > 0$. When Case II occurs, if $b \in (b_0, b_1) \bigcup (b_2, b_3)$, then $H_{2,0} > 0$.

When $b > b_0$, we can see that $A_3 > 0$. So if $b > b_0$, $H_{2,0} > 0$ and $A_1 d_1 + A_2 d_2 \geq 0$, then $H_{2,n} > 0$ for $n \in \mathbb{N}_0$.

When $A_2 > 0$, if the diffusion coefficient d_2 is sufficiently large relative to the diffusion coefficient d_1, then $A_1 d_1 + A_2 d_2 \geq 0$ can be established.

It is easy to see that if $\frac{rbc^2}{a(b-1)^2} - \frac{rc(ab-a-c)}{a(b-1)(rc+ab-a)} > 0$, then $A_2 > 0$. $\frac{rbc^2}{a(b-1)^2} - \frac{rc(ab-a-c)}{a(b-1)(rc+ab-a)} > 0$, is equivalent to

$$a(c-a)b^2 + (rc^2 + 2a^2)b - a(c+a) > 0. \tag{15}$$

When $c = a$, the (15) always holds since $b > b_0$. When $c \neq a$, the equation $a(c-a)b^2 + (rc^2 + 2a^2)b - a(c+a) = 0$ has two real roots

$$b_{4,5} = \frac{-(rc + 2a^2) \pm \sqrt{r^2c^2 + 4ra^2 + 4a^2}}{2a(c-a)}.$$

If $c > a$, $b_5 < 0 < b_4$ and the (15) holds when $b > b_4$ or $b < b_5$. If $c < a$, $0 < b_4 < b_5$ and the (15) hold when $b_4 < b < b_5$.

Through calculation, we get $A_2 = \frac{a_3 y^3 + a_2 y^2 + a_1 y + a_0}{a^2 y^2 (ay + rc)}$, where

$$\begin{aligned} a_0 &= (r + 2a)c^3 r^2 > 0, \\ a_1 &= (3r + 2cr + 4a)ac^2 r > 0, \\ a_2 &= [(1-r)a + 3(c+1)r]a^2 c, \\ a_3 &= (c+1)a^3 > 0, \\ y &= b - 1. \end{aligned}$$

If $r \leq 1$ or $a \leq 3(c+1)$, then $a_2 > 0$. When $r > 1$ and $a > 3(c+1)$, $a_2 > 0$ if and only if $r < \frac{a}{a-3(c+1)}$. Obviously, if $a_2 > 0$, then $A_2 > 0$ for $b > b_0$.

From the above discussion and Lemma 3.5, we reach the following conclusions.

Corollary 3.6 *In Case I, if one of the following conditions holds*

(1) $c > a$, $\max\{b_0, b_4\} < b < b_1$,
(2) $c < a$, $\max\{b_0, b_4\} < b < \min\{b_1, b_5\}$,
(3) $c = a$, $b_0 < b < b_1$, *and* $\frac{d_2}{d_1} > -\frac{A_1}{A_2}$, *then the spatially uniform positive steady state* E^* *of the system* (5) *is locally asymptotically stable when* $\tau = 0$.

Corollary 3.7 *In Case II, if one of the following conditions holds*

(1) $c > a$, $\max\{b_0, b_4\} < b < b_1$ *or* $\max\{b_2, b_4\} < b < b_3$,
(2) $c < a$, $\max\{b_0, b_4\} < b < \min\{b_1, b_5\}$ *or* $\max\{b_2, b_4\} < b < \min\{b_3, b_5\}$,
(3) $c = a$, $b_0 < b < b_1$ *or* $b_2 < b < b_3$, *and* $\frac{d_2}{d_1} > -\frac{A_1}{A_2}$, *then the spatially uniform positive steady state* E^* *of system* (5) *is locally asymptotically stable when* $\tau = 0$.

Corollary 3.8 *Suppose* $b > b_0$. *If one of the following conditions holds*

(1) $r \leq 1$,

(2) $a \le 3(c+1)$,
(3) $a > 3(c+1)$ *and* $1 < r < \frac{a}{a-3(c+1)}$ *and* $\frac{d_2}{d_1} > -\frac{A_1}{A_2}$, *then the spatially uniform positive steady state* E^* *of system* (5) *is locally asymptotically stable when* $\tau = 0$.

Now, we assume the condition $(\mathcal{H})$ holds, we would like to seek critical value τ such that there exists a pair of purely imaginary eigenvalue. Let $\mathrm{i}\omega(\omega > 0)$ be the solution of the $(n+1)$th equation of (13), we have

$$-\mathrm{i}\omega^3 - a_{2,n}\omega^2 + \mathrm{i}a_{1,n}\omega + a_{0,n} + (\mathrm{i}b_{1,n}\omega + b_{0,n})(\cos\omega\tau - \mathrm{i}\sin\omega\tau) = 0.$$

Separating the real and imaginary parts gives

$$\begin{cases} -\omega^3 + a_{1,n}\omega = b_{0,n}\sin\omega\tau - b_{1,n}\omega\cos\omega\tau, \\ a_{2,n}\omega^2 - a_{0,n} = b_{0,n}\cos\omega\tau + b_{1,n}\omega\sin\omega\tau. \end{cases} \tag{16}$$

Square each sides of (16) and plus, we have

$$\omega^6 + f_n\omega^4 + g_n\omega^2 + h_n = 0 \tag{17}$$

where $f_n = a_{2,n}^2 - 2a_{1,n}$, $g_n = a_{1,n}^2 - 2a_{2,n}a_{0,n} - b_{1,n}^2$, $h_n = a_{0,n}^2 - b_{0,n}^2$.

Let $z = \omega^2$, then (17) becomes

$$P_n(z) = z^3 + f_n z^2 + g_n z + h_n = 0. \tag{18}$$

Lemma 3.9 *For Eq.* (18), *we have the following conclusions.*

(i) *If* $h_n < 0$, *Eq.* (18) *has at least one positive roots.*
(ii) *If* $h_n \ge 0$ *and* $f_n^2 - 3g_n \le 0$, *Eq.* (18) *has no positive root.*
(iii) *If* $h_n \ge 0$ *and* $f_n^2 - 3g_n > 0$, *Eq.* (18) *has positive roots if and only if* $z_{1,n}^* > 0$ *and* $P(z_{1,n}^*) \le 0$, *where* $z_{1,n}^* = \frac{-f_n + \sqrt{f_n^2 - 3g_n}}{3}$.

Proof Since $P_n(z) \to +\infty$ as $z \to +\infty$, we conclude that $P_n(z)$ has at least one positive root if $P_n(0) = h_n < 0$. Differentiating $P_n(z)$ with respect to z, we have $P_n'(z) = 3z^2 + 2f_n z + g_n$. If $f_n^2 - 3g_n \le 0$, then $P_n'(z) \ge 0$ and $P_n(z)$ is nondecreasing when $z \ge 0$. Thus, for $h_n \ge 0$ and $f_n^2 - 3g_n \le 0$, the Eq. (18) has no positive root. When $h_n \ge 0$ and $f_n^2 - 3g_n > 0$, $P_n'(z)$ has two roots $z_{1,n}^* = \frac{-f_n + \sqrt{f_n^2 - 3g_n}}{3}$ and $z_{2,n}^* = \frac{-f_n - \sqrt{f_n^2 - 3g_n}}{3}$. Clearly,

$$p_n''(z_{1,n}^*) = 2\sqrt{f_n^2 - 3g_n} > 0, \quad p_n''(z_{2,n}^*) = -2\sqrt{f_n^2 - 3g_n} < 0.$$

So $z_{1,n}^*$ is the locally minimum point of $P_n(z)$, and $z_{2,n}^*$ is the locally maximum point of $P_n(z)$. Noticing that $h_n \ge 0$, $z_{1,n}^*$ is the local minimum of $P_n(z)$ and $P_n(z) \to +\infty$ as $z \to +\infty$, we know that the sufficiency of (iii) is true. In what follows, we need to prove the necessity of (iii). Suppose that either $z_{1,n}^* \le 0$ or $z_{1,n}^* > 0$ and $P_n(z_{1,n}^*) > 0$.

Since $P_n(z)$ is increasing for $z \geq 0$ and $P_n(0) = h_n \geq 0$, we know that $P_n(z)$ has no positive real roots for $z^*_{1,n} \leq 0$. If $z^*_{1,n} > 0$ and $P_n(z^*_{1,n}) > 0$, since $h(x^*_1)$ is the local minimum value, it follows that $P_n(0) = h_n > 0$ that when $z^*_{1,n}$ and $P_n(z^*_{1,n}) > 0$, $P_n(z)$ has no positive real roots, too. This proves the lemma. □

Corollary 3.10 *If* $b_0 < b < b_6 = 1 + \frac{3c}{2a} + \frac{\sqrt{9c^2+8ac}}{2a}$, *then* $h_0 < 0$.

Proof When $b > b_0$, we have $a_{0,0} + b_{0,0} > 0$. So $h_0 = a^2_{0,0} - b^2_{0,0} = (a_{0,0} + b_{0,0})(a_{0,0} - b_{0,0}) < 0$ if $a_{0,0} - b_{0,0} < 0$ and $b > b_0$.

$$\begin{aligned} a_{0,0} - b_{0,0} &= \frac{2rbc^2}{a(b-1)^2} - \frac{rc(ab-a-c)(ab+rc+a)}{(b-1)(rc+ab-a)} \\ &= \frac{rc}{a(b-1)}\left(\frac{2bc}{b-1} - (ab-a-c) - \frac{2a(ab-a-c)}{rc+ab-a}\right) \end{aligned}$$

If $b > b_0$ and $\frac{2bc}{b-1} - (ab-a-c) < 0$, then $a_{0,0} - b_{0,0} < 0$. When $b > b_0$,

$$\begin{aligned} &\frac{2bc}{b-1} - (ab-a-c) < 0 \\ &\quad \Leftrightarrow ab^2 - (2a+3c)b + a + c > 0 \\ &\quad \Leftrightarrow 1 + \frac{3c}{2a} - \frac{\sqrt{9c^2+8ac}}{2a} < b < 1 + \frac{3c}{2a} + \frac{\sqrt{9c^2+8ac}}{2a}. \end{aligned}$$

Because of $1+\frac{3c}{2a} - \frac{\sqrt{9c^2+8ac}}{2a} < b_0 < 1+\frac{3c}{2a} + \frac{\sqrt{9c^2+8ac}}{2a}$, we get $h < 0$ if $b_0 < b < b_6$. □

Denote

$$\mathcal{D} = \{n \in \mathbb{N}_0 : h_n < 0;\ \text{or } h_n \geq 0,\ f_n^2 - 3g_n > 0,\ z^*_{1,n}0,\ \text{and } P_n(z^*_{1,n}) \leq 0\}.$$

From Lemma 3.9, we know that Eq. (18) has positive roots if and only if $n \in \mathcal{D}$. Without loss of generality, we assume Eq. (18) has three positive roots $z_{1,n}$, $z_{1,n}$ and $z_{3,n}$ when $n \in \mathcal{D}$. We denote $\omega_{k,n} = \sqrt{z_{k,n}}$ and

$$\tau^{(j)}_{k,n} = \begin{cases} \frac{1}{\omega_{k,n}}\left[\arccos \frac{b_{0,n}(a_{2,n}\omega^2_{k,n} - a_{0,n}) + b_{1,n}\omega_{k,n}(\omega^2_{k,n} - a_{1,n}\omega_{k,n})}{b^2_{1,n}\omega + k,n^2 + b^2_{0,n}} + 2j\pi\right], & \sin\omega_{k,n}\tau^{(0)}_{k,n} \geq 0, \\ \frac{1}{\omega_{k,n}}\left[-\arccos \frac{b_{0,n}(a_{2,n}\omega^2_{k,n} - a_{0,n}) + b_{1,n}\omega_{k,n}(\omega^2_{k,n} - a_{1,n}\omega_{k,n})}{b^2_{1,n}\omega + k,n^2 + b^2_{0,n}} + 2(j+1)\pi\right], & \sin\omega_{k,n}\tau^{(0)}_{k,n} < 0, \end{cases}$$

for $k = 1, 2, 3$, $j \in \mathbb{N}_0$ and $n \in \mathcal{D}$. When $\tau = \tau^{(j)}_{k,n}$, Eq. (13) has a pair of purely imaginary roots $\pm i\omega_{k,n}$.

For some $n \in \mathcal{D}$, let $\lambda(\tau) = \alpha_n(\tau) + i\omega$ be a root of the $(n+1)$th equation of (13) which satisfies $\omega_n(\tau^{(j)}_{k,n}) = \omega_{k,n}$ and $\alpha_n(\tau^{(j)}_{k,n}) = 0$ for $k = 1, 2, 3$ and $j \in \mathbb{N}_0$.

Lemma 3.11 *sign*$\{\alpha_n'(\tau_{k,n}^{(j)})\} = sign\{P_n'(z_{k,n})\}$.

Proof Differentiating the both side of Eq. (13) with respect to τ, it follows that

$$\left(\frac{\mathrm{d}\lambda}{\mathrm{d}\tau}\right)^{-1} = \frac{(3\lambda^2 + 2a_{2,n}\lambda + a_{1,n})\mathrm{e}^{\lambda\tau}}{\lambda(b_{1,n}\lambda + b_{0,n})} + \frac{b_{1,n}}{\lambda(b_{1,0}\lambda + b_{0,n})} - \frac{\tau}{\lambda}.$$

From (16), we have

$$\alpha_n'(\tau_{k,n}^{(j)})^{-1} = \mathrm{Re}\left(\frac{\mathrm{d}\lambda}{\mathrm{d}\tau}\right)^{-1}\Big|_{\tau=\tau_{k,n}^{(j)}} = \frac{P_n'(z_{k,n})}{b_{1,n}^2\omega_{k,n}^2 + b_{0,n}^2}.$$

This proves the lemma. □

Let

$$\tau^* = \tau_{k_0,n_0}^{(0)} = \min_{k=1,2,3,\ n\in\mathcal{D}}\{\tau_{k,n}^{(0)}\}.$$

From Lemma 3.5, 3.9 and 3.11, we have the following conclusion.

Theorem 3.12 *Suppose the condition* $(\mathcal{H})$ *holds.*

(i) *If* $h \geq 0,\ f_n^2 - 3g_n \leq 0$, *or* $f_n^2 - 3g_n > 0,\ z_{1,n}^* < 0$, *or* $f_n^2 - 3g_n > 0,\ z_{1,n}^* > 0,\ P_n(z_{1,n}^*) > 0$ *for all* $n \in \mathbb{N}_0$, *the spatially uniform steady state* E^* *of the system* (5) *is locally asymptotically stable for all* $\tau > 0$.

(ii) *If* $h_n < 0$, *or* $h_n \geq 0,\ f_n^2 - 3g_n > 0,\ z_{1,n}^* > 0$ *and* $P_n(z_{1,n}^*) \leq 0$ *for some* $n \in \mathbb{N}_0$, *the spatially uniform steady state* E^* *of the system* (5) *is locally asymptotically stable for* $\tau \in [0, \tau^*)$.

(iii) *If all conditions as stated in (ii) and* $P_n'(z_{k,n}) \neq 0$ *hold, the system* (5) *undergoes a Hopf bifurcation at* E^* *when* $\tau = \tau_{k,n}^{(j)},\ k = 1, 2, 3,\ j \in \mathbb{N}_0$.

4 Numerical Simulations

For the convenience of presentation, our numerical simulations are performed for the tumor site as a domain in $\mathbb{R}^2$. We describe briefly the numerical method; we use to solve the system (5) at the end of "Appendix". In the following, we demonstrate several typical cases which correspond to our analysis.

Let $\Omega = (0, \pi) \times (0, \pi)$ (i.e., $p = q = 1$) and choose

$$r = 0.1, a = 0.01, c = 0.08, d_1 = 0.02, d_2 = 0.2.$$

For this set of parameter values, we can get $b_0 = 1 + \frac{c}{a} = 9,\ b_1 \approx 135.5540$. And when $9 < b < 135.5540$, (H) holds. So when $\tau = 0$, the positive steady state E^* is stable if $9 < b < 135.5540$. From our calculation, we find only for $b \geq 24.4105$ and

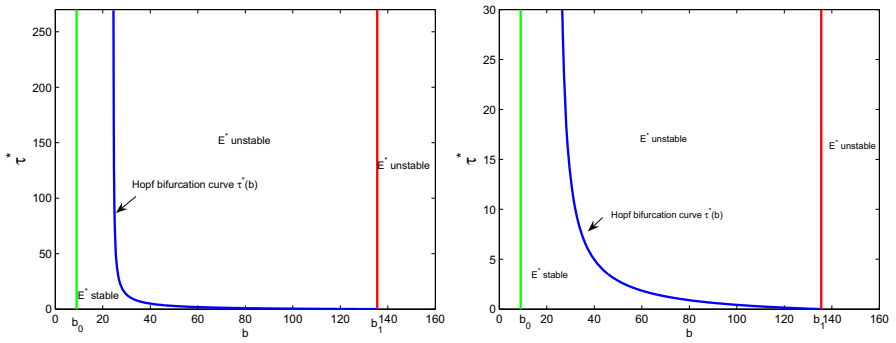

Fig. 1 A bifurcation curve $\tau^*(b)$ (Colour figure online)

$n = 0$, (17) has a positive root, and we get a bifurcation curve about τ^* and b (see Fig. 1).

If we choose

$$r = 0.1, a = 0.01, b = 4, c = 0.08, d_1 = 0.02, d_2 = 0.2, \tau = 2.$$

For this set of parameter values, we observe that $b < 1 + \frac{c}{a}$. So from Theorem 3.4, the steady state $E_1 = (1, 0, 0)$ is globally asymptotically stable (see Fig. 2). The initial conditions of Fig. 3 are $u(x,t) = 0.5000 + 0.3000\cos 2x \cos y$, $w(x,t) = 0.0500 + 0.0300\cos 2x \cos y$, $v(x,t) = 8.0000 + 2.0000\cos 2x \cos y$, $(x, y, t) \in [0, \pi] \times [0, \pi] \times [-\tau, 0]$. In Fig. 2, we take $x = \pi/3$ and $y = \pi/3$, respectively.

If we chose $b = 60$, then by calculation, we have

$$\omega_{1,0} = \approx 0.0743, \ \tau_{1,0}^{(j)} + \approx 1.8518 + 84.5804j, \quad \text{for} j \in \mathbb{N}_0.$$

So $\tau^* = \tau_{1,0}^{(0)} \approx 1.8518$. Furthermore, from "Appendix", we have $c_1(0) \approx -0.5369 - 2.2209\text{i}$, $P'(\omega_{1,0}^2) = 0.0118 > 0$. From Theorem 3.12 and "Appendix", we know that positive equilibrium $E^* = (0.1356, 0.0116, 8.5284)$ is locally asymptotically stable when $\tau \in [0, \tau^*)$ (see Fig. 3), and the direction of the Hopf bifurcation is supercritical when $\tau = \tau^*$, that is the bifurcating periodic solutions exist for $\tau > \tau^*$, and they are orbitally stable (see Fig. 4). The initial conditions of Fig. 3 are $u(x,t) = 0.1356 + 0.1000\cos 2x \cos y$, $w(x,t) = 0.0116 + 0.0100\cos 2x \cos y$, $v(x,t) = 8.5284 + 3.0000\cos 2x \cos y$, $(x, y, t) \in [0, \pi] \times [0, \pi] \times [-\tau, 0]$ and the initial conditions of Fig. 4 are $u(x,t) = 0.2000 + 0.1000\cos 2x \cos y$, $w(x,t) = 0.0200 + 0.0100\cos 2x \cos y$, $v(x,t) = 8.5000 + 3.0000\cos 2x \cos y$, $(x, y, t) \in [0, \pi] \times [0, \pi] \times [-\tau, 0]$. In Fig. 3 and Fig. 3, we take $x = \pi/3$ and $y = \pi/3$, respectively.

5 Conclusion and Discussion

Incorporating virus diffusivity, tumor cell diffusion, and the viral lytic cycle into a basic oncolytic virus dynamics model, we formulate a mathematical model in terms of delay

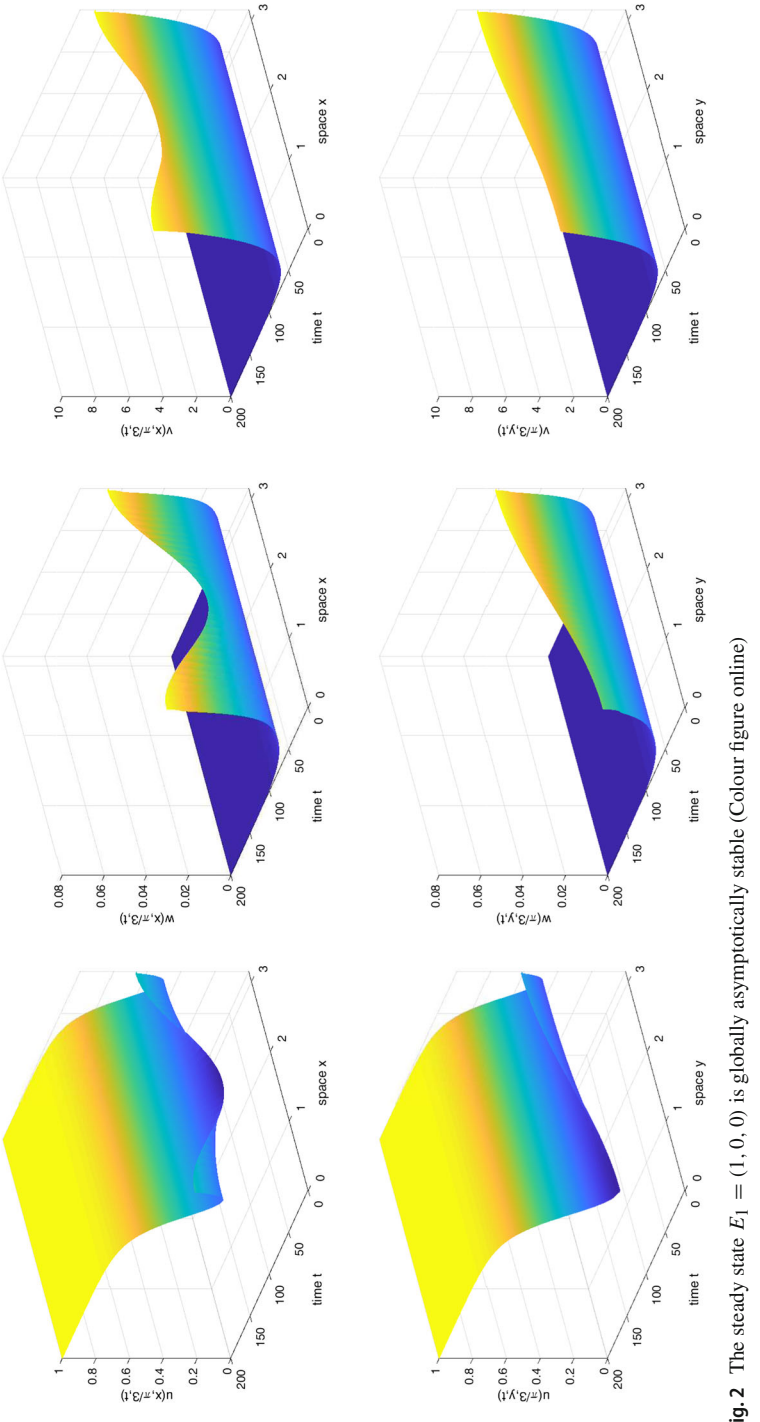

Fig. 2 The steady state $E_1 = (1, 0, 0)$ is globally asymptotically stable (Colour figure online)

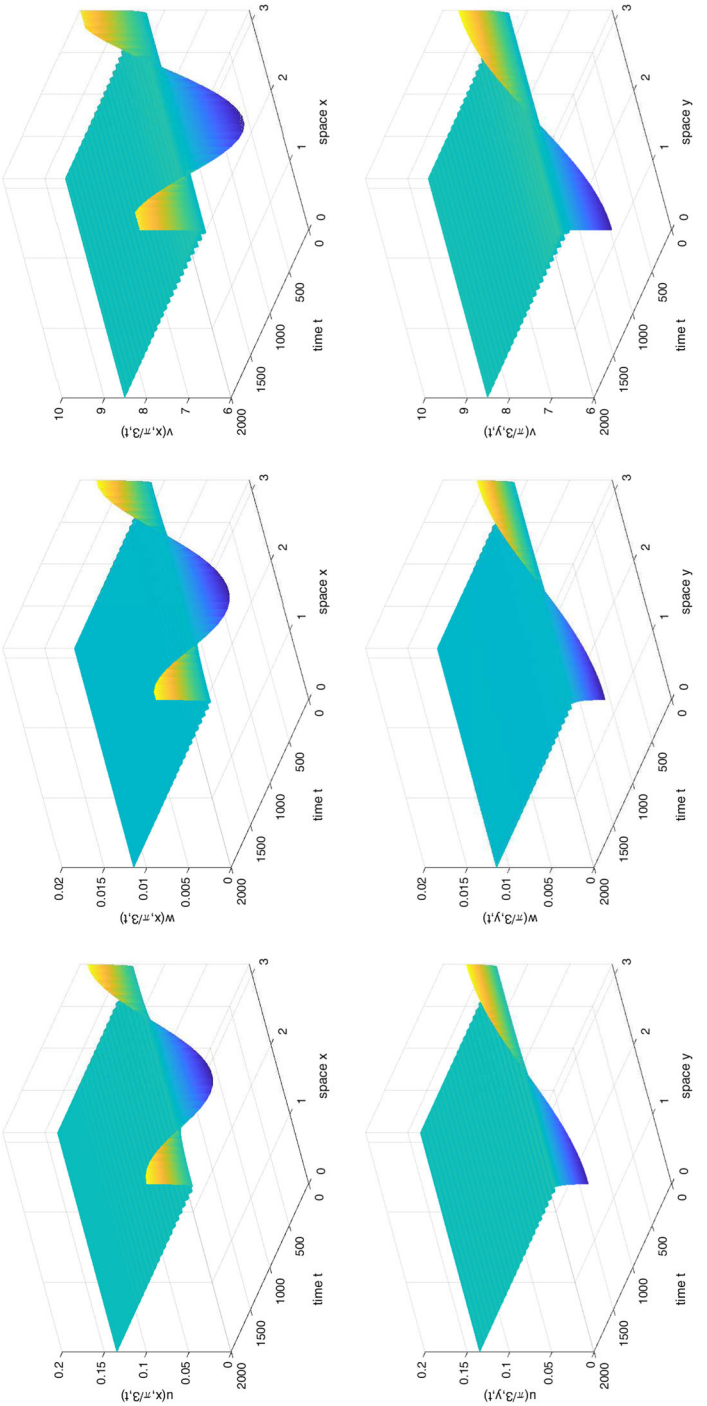

Fig. 3 The positive equilibrium is asymptotically stable when $\tau \in [0, \tau^*)$, where $\tau = 0.9 < \tau^* \approx 1.8518$ (Colour figure online)

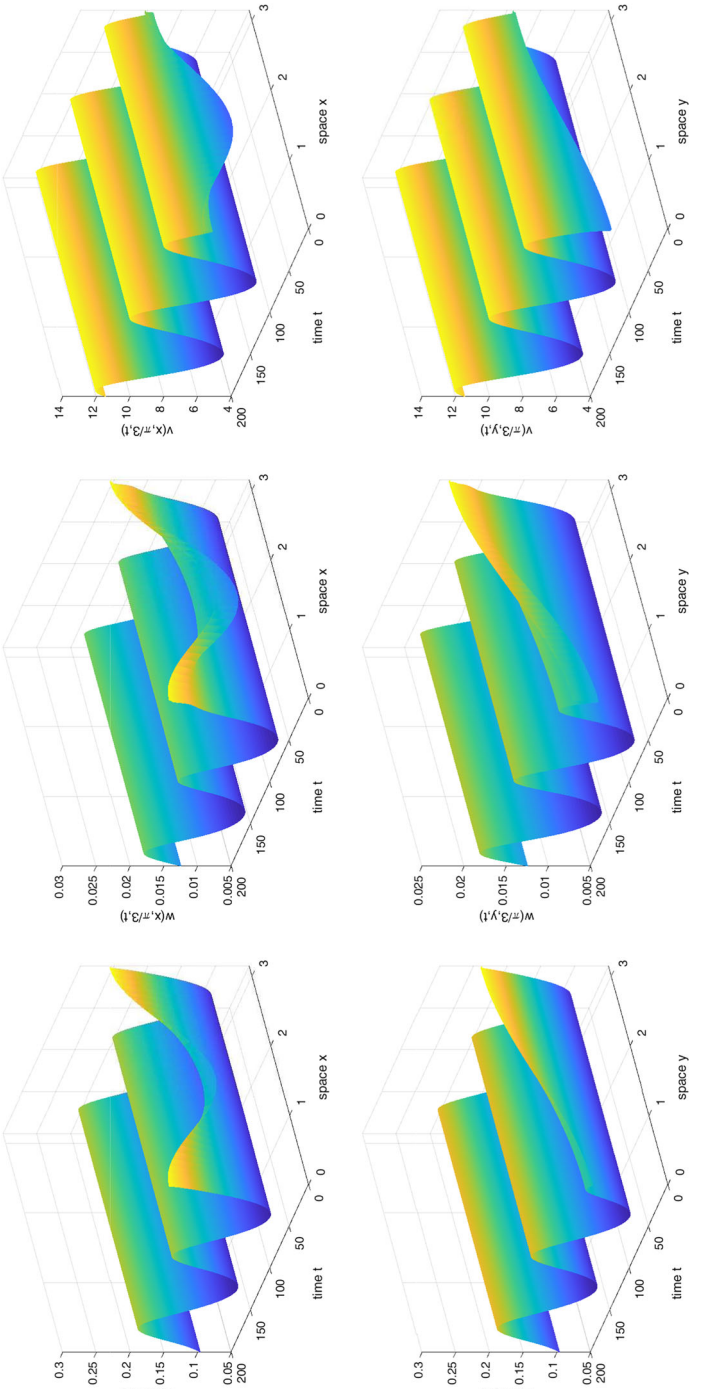

Fig. 4 The bifurcating periodic solution is stable, where $\tau = 2 > \tau^* \approx 1.8518$ (Colour figure online)

partial differential equations for oncolytic virotherapy. We conduct a detailed study of the dynamics of our model. We find the positive invariant domain for the omega limit set and three spatially uniform equilibrium solutions of our model. Comparing with the basic models without diffusions of virus and tumor cells and the delay of the viral lytic cycle, we find a first critical value of the viral burst size, and when the viral burst size is smaller than this first critical value, the spatially uniform virus-free steady state is globally asymptotically stable for any viral lytic period delay and any diffusion coefficients of tumor cells and viruses. When the viral burst size is greater than the first critical value, we characterize the stability of the spatially uniform positive steady state by three major parameters: the ratio of virus diffusion coefficient to that of tumor cells, the length of the viral lytic cycle, and the viral burst size with six different values that are greater than the first critical value. These results are summarized in Lemma 3.5 with Corollaries 3.6, 3.7, and 3.8; lemma 3.9 with Corollary 3.10, Lemma 3.11; and Theorem 3.12. These detailed information cannot be obtained from the models without diffusions of virus and tumor cells and delays of viral lytic cycle. For instant, if we don't consider the viral lytic cycle meaning the viral lytic cycle length is zero, in order to have a locally asymptotical stability of the spatially uniform positive steady state, the ratio between diffusion coefficients must be greater than a particular value and the viral burst size must be greater than the first critical value but smaller than other values depending on the tumor growth rate and virus clearance rate. If we consider the viral lytic cycle as a delay parameter, we find a critical value for the length of the viral lytic cycle. Combining conditions for the ratio between diffusion coefficients and viral burst size, the spatially uniform positive steady state is locally asymptotical stable when the viral lytic cycle length is smaller than the critical value while the system undergoes Hopf bifurcation at the critical value of the viral lytic cycle length and has stable periodic solutions when the viral lytic cycle length is greater than the critical value. For these results, we give some biological implications as follows.

From our analysis, we know that the parameters including the viral burst size, the viral lytic cycle, and the diffusion coefficients of viruses and cells play important roles in the dynamics of oncolytic viral therapy. Our model has three spatially homogeneous equilibrium solutions, E_0, E_1, and E^* which are related to long-term behaviors of general solutions. They may have some medical implications. It is reasonable that the zero solution E_0 is always unstable for any parameter values since the tumor always grows in its beginning. Theorem 3.4 gives a critical value for the viral burst size, and below that value, the viral therapy fails no matter what values of any other parameters are chosen. This confirms that the potency of oncolytic viruses is important, and the viral burst size greater than that critical value is necessary condition for the treatment to work. It is hoped oncolytic viruses will eradicate the tumor completely. However, this is not always the case. When viruses cannot completely eradicate the tumor, we may hope the virus treatment will be stabilized at a level where the tumor cells, infected tumor cells, and viruses are constant. We find some conditions under which the viral therapy can be stabilized. Under the condition $(\mathcal{H})$ which includes the viral burst size is greater than the critical value and the ratio of virus diffusion coefficient to cell diffusion coefficient is greater than certain values in Corollary 3.6–3.8, and the condition states in Theorem 3.12, the spatially uniform

equilibrium solution E^* which is constant solution is stable. We also obtain a critical value of the viral lytic cycle below that value E^* is stable while at that value point, the system undergoes a Hopf bifurcation. Spatially homogeneous periodic solutions arise from Hopf bifurcations. We numerically show these periodic solutions are stable. We may consider the stable spatially homogeneous periodic solution as one type of treatment stabilization. In addition, we find a functional relationship between the viral burst size and lytic cycle shown in Fig. 1 which may implicate that the viral lytic cycle length will change if the viral burst size changes. Since we can genetically change viral genome for different burst sizes, we accordingly change their lytic cycles. As long as the condition in Theorem 3.12 is satisfied, the stabilization of treatments can be achieved.

As mentioned in introduction, there have been many studies on oncolytic virotherapy experimentally and theoretically. Recently, Wodarz et al. (2012) have conducted an *in vitro* experiment with recombinant adenovirus type-5 in a two-dimensional setting and used an agent-based stochastic computational model to simulate experimental observations. They observed three spatial patterns, "hollow ring structure", "filled ring structure, and "disperse pattern". They found that both the filled ring structure and disperse pattern of initial expansion were indicative of treatment failure. The hollow ring structure was associated with either target cell extinction or low-level persistence, both of which can be viewed as treatment success. It seems that the filled ring structure and disperse pattern correspond to the spatial positive steady state in our model, and the hollow ring structure corresponds the spatial virus-free steady state in our model. However, our study gives more detailed information about the spatial positive equilibriums and possibilities of stable periodic behaviors of the spatial patterns. They also found that equilibrium properties of ordinary differential equations describing the dynamics in local neighborhoods in the agent-based model can predict the outcome of the spatial virus-cell dynamics. This finding agrees with our results since our model is based on local interactions. A more recent study by Wang et al. (2017) incorporated nonlocal reaction terms in their delay reaction–diffusion system for oncolytic virotherapy. They gave different treatment strategies according to different gene mutations, which has theoretical interests. Friedman and Lai (2018) presented a computational study about combination therapy for cancer with oncolytic virus and checkpoint inhibitor. This study did not focus on spatial patterns of oncolytic virus spreading within tumors. Timalsina et al. (2017) proposed a detailed reaction–diffusion model for virotherapy and conducted a computational study. This model focused on the different functions of innate and adaptive immune systems in oncolytic viral therapies.

It is clear that our model incorporates basic components of oncolytic viral therapy although it reveals important features of oncolytic viral therapy. There are several components which are not included, for example immune cells. The immune system has two different functions in oncolytic viral therapies. The immune cells can be incorporated to our model. However, it is beyond the scope of our current work. This may be considered in our future study.

Acknowledgements JZ and JPT would like to acknowledge the support from U54CA132383 of NIH (awarded to JPT), Fundamental Research Funds for the Universities in Heilongjiang Province (No:

RCCX201718, awarded to JZ) and Fundamental Research Funds of Education Department of Heilongjiang Province (No: 135109228, awarded to JZ). The authors would like to acknowledge the suggestion of model formulation from Philip K. Maini. The authors would like to thank two anonymous reviewers for their insightful comments and constructive suggestions which greatly help in improving the presentation of our results.

Appendix: Stability and Direction of the Hopf Bifurcations

Theory of functional reaction–diffusion systems says that a family of spatially homogeneous or inhomogeneous periodic solutions may bifurcate from the positive homogeneous equilibrium state E^* of the system (5) when τ crosses through the critical value τ^*. In Appendix, we investigate the stability and direction of Hopf bifurcations by using the center manifold theorem and the normal formal theory of partial functional differential equation (Faria 2000; Wu 2012). Basically, the system (5) firstly is represented as an abstract ODE system. Secondly, at the center manifold of the ODE system corresponding to E^*, the normal form or Taylor expansion of the ODE system is computed. Then, the coefficients of the first four terms of the normal form will reveal all the properties of the periodical solutions (Hassard et al. 1981). At the end, we briefly describe the numerical method we use to solve our system.

Let $u_1(\cdot,t) = u(\cdot,\tau t) - u^*,\ u_2(\cdot,t) = w(\cdot,\tau t) - w^*,\ u_3(\cdot,t) = v(\cdot,\tau t) - v^*$ and $U(t) = (u_1(\cdot,t), u_2(\cdot,t), u_3(\cdot,t))^T$. Then, the system (5) can be written as an equation in the function space $\mathscr{C} = C([-1,0], X)$:

$$\frac{\mathrm{d}U(t)}{\mathrm{d}t} = \tau D\Delta U(t) + L(\tau)(U_t) + f(U_t,\tau), \tag{19}$$

where $D = \mathrm{diag}(d_1, d_1, d_2)$, $L(\tau)(\cdot) : \mathscr{C} \to X$ and $f : \mathscr{C} \times \mathbb{R} \to X$ are given, respectively, by

$$\begin{aligned} L(\tau)(\varphi) &= \tau L_1\varphi(0) + \tau L_2\varphi(-1),\\ f(\varphi,\tau) &= \tau(f_1(\varphi,\tau),\ f_2(\varphi,\tau),\ f_3(\varphi,\tau))^T, \end{aligned}$$

with

$$\begin{aligned} f_1(\varphi,\tau) &= -r\varphi_1^2(0) - r\varphi_1(0)\varphi_2(0) - a\varphi_1(0)\varphi_3(0),\\ f_2(\varphi,\tau) &= a\varphi_1(-\tau)\varphi_3(-\tau),\\ f_3(\varphi,\tau) &= -a\varphi_1(0)\varphi_3(0), \end{aligned}$$

for $\varphi = (\varphi_1,\varphi_2,\varphi_3)^{\mathrm{T}} \in \mathscr{C}$.

Let $\tau = \tau^* + \sigma$, then (19) can be rewritten as

$$\frac{\mathrm{d}U(t)}{\mathrm{d}t} = \tau^* D\Delta U(t) + L(\tau^*)(U_t) + F(U_t,\sigma), \tag{20}$$

where

$$F(\varphi, \sigma) = \sigma D\Delta\varphi(0) + L(\sigma)(\varphi) + f(\varphi, \tau^* + \sigma),$$

for $\varphi \in \mathscr{C}$.

From the previous subsection, when $\sigma = 0$ (i.e. $\tau = \tau^*$) the system (20) undergoes Hopf bifurcation at the equilibrium $(0, 0, 0)$, it is also clear that $\pm i\omega^*\tau^*$ are simply purely imaginary eigenvalues of the linearized system of (20) at the origin

$$\frac{dU(t)}{dt} = (\tau^* + \sigma)D\Delta U(t) + L(\tau^* + \sigma)(U_t), \tag{21}$$

with $\sigma = 0$ and all other eigenvalues of (21) at $\sigma = 0$ have negative real parts.

The eigenvalues of $\tau D\Delta$ on X are $-\tau d_1\mu_n$ (the number of multiples is two) and $-\tau d_2\mu_n$, $n \in \mathbb{N}_0$, with corresponding eigenfunctions $\beta_n^1(x) = (\gamma_n(x), 0, 0)^T$, $\beta_n^2(x) = (0, \gamma_n(x), 0)^T$ and $\beta_n^3(x) = (0, 0, \gamma_n(x))^T$, where $\gamma_n(x) = \frac{\phi_n(x)}{(\int_\omega \phi_n(x)dx)^{\frac{1}{2}}}$.

We have that the solution operator of (21) is a C_0 semigroup, and the infinitesimal generator A_σ is given by

$$A_\sigma\phi = \begin{cases} \dot{\phi}(\theta), & \theta \in [-r, 0), \\ D\Delta\phi(0) + L(\tau^* + \sigma)(\phi), & \theta = 0. \end{cases} \tag{22}$$

and the domain $\mathrm{dom}(A_\sigma)$ of A_σ is

$$\mathrm{dom}(A_\sigma) := \{\phi \in \mathscr{C} : \dot{\phi} \in \mathscr{C}, \phi(0) \in \mathrm{dom}(\Delta), \dot{\phi}(0) = D\Delta\phi(0) + L(\tau^* + \sigma)(\phi)\}.$$

Hence, Eq. (20) can be rewritten as the abstract ODE in $\mathscr{C}$:

$$\dot{U}_t = A_\sigma U_t + R(\sigma, U_t), \tag{23}$$

where

$$R(\sigma, U_t)(\theta) = \begin{cases} 0, & \theta \in [-1, 0), \\ F(\sigma, U_t), & \theta = 0. \end{cases}$$

We denote

$$\beta_n = \{(1, 0, 0)^{\mathrm{T}}\gamma_n, (0, 1, 0)^{\mathrm{T}}\gamma_n, (0, 0, 1)^{\mathrm{T}}\gamma_n\}.$$

For $\phi = (\phi^{(1)}, \phi^{(2)})^T \in \mathscr{C}$, we denote

$$\phi_n = \langle \phi, \beta_n \rangle = \left(\langle \phi^{(1)}, \gamma_n \rangle, \langle \phi^{(2)}, \gamma_n \rangle, \langle \phi^{(3)}, \gamma_n \rangle \right)^{\mathrm{T}}.$$

Define $A_{\sigma,n}$ as

$$A_{\sigma,n}(\phi_n(\theta)\gamma_n) = \begin{cases} \dot{\phi}_n(\theta)\gamma_n, & \theta \in [-1, 0), \\ \int_{-r}^{0} \mathrm{d}\eta_n(\sigma, \theta)\phi_n(\theta)\gamma_n, & \theta = 0. \end{cases} \tag{24}$$

Furthermore, we have

$$L_{\sigma,n}(\phi_n) = (\tau^* + \sigma)L_1\phi_n(0) + (\tau^* + \sigma)L_2\phi_n(-1),$$

and

$$-\mu_n D\phi_n(0) + L_{\sigma,n}(\phi_n) = \int_{-1}^{0} \mathrm{d}\eta_n(\sigma, \theta)\phi_n(\theta),$$

where

$$\eta_n(\sigma, \theta) = \begin{cases} -(\tau^* + \sigma)L_2, & \theta = -1, \\ 0, & \theta \in (-1, 0), \\ (\tau^* + \sigma)(L_1 - \mu_n D), & \theta = 0. \end{cases}$$

Define $\mathscr{C}^* = C([0, 1]; X)$ and a bilinear form $(\cdot, \cdot)$ on $\mathscr{C}^* \times \mathscr{C}$

$$(\psi, \phi) = \sum_{k,j=0}^{\infty} (\psi_k, \phi_j)_c \int_{\Omega} \gamma_k \gamma_j \mathrm{d}x,$$

where $(\cdot, \cdot)_c$ is the bilinear form defined on $C^* \times C$

$$(\psi_n, \phi_n)_c = \overline{\psi}_n^T(0)\phi_n(0) - \int_{-1}^{0} \int_{\xi=0}^{\theta} \overline{\psi}_n^T(\xi - \theta)\mathrm{d}\eta_n(0, \theta)\phi_n(\xi)\mathrm{d}\xi,$$

and

$$\psi = \sum_{n=0}^{\infty} \psi_n\gamma_n \in \mathscr{C}^*, \ \phi = \sum_{n=0}^{\infty} \phi_n\gamma_n \in \mathscr{C},$$

with

$$\phi_n \in C = C([-1, 0], \mathbb{R}^2), \ \ \psi_n \in C^* = ([0, 1], \mathbb{R}^2).$$

Notice that

$$\int_{\Omega} \gamma_k \gamma_j \mathrm{d}x = 0 \ \text{ for } \ k \neq j,$$

we have

$$(\psi, \phi) = \sum_{n=0}^{\infty} (\psi_n, \phi_n)_c,$$

We define the adjoint operator A^* of A_0

$$A^*\psi(s) = \begin{cases} -\dot{\psi}(s), & s \in (0, 1], \\ \sum_{n=0}^{\infty} \int_{-1}^{0} \mathrm{d}\eta_n^T(0, t)\psi_n(-t)\gamma_n, & s = 0. \end{cases}$$

Let

$$q(\theta)\gamma_{n_0} = q(0)e^{i\omega^*\tau^*\theta}\gamma_{n_0},\ q^*(s)\gamma_{n_0} = q^*(0)e^{i\omega^*\tau^*s}\gamma_{n_0}$$

be the eigenfunctions of A_0, and A^* corresponds to $i\omega^*\tau^*$ and $-i\omega^*\tau^*$, respectively. By direct calculations, we chose

$$q(0) = (1, C_1, C2)^{\mathrm{T}},\ q^*(0) = M(1, C_3, C_4)^{\mathrm{T}}$$

where

$$\begin{aligned} C_1 &= \frac{a^2u^*v^* - (\mathrm{i}\omega^* + d_1\mu_{n_0} + ru^*)(\mathrm{i}\omega^* + d_2\mu_{n_0} + au^* + c)}{abu^* + ru^*(\mathrm{i}\omega^* + d_2\mu_{n_0} + au^* + c)}, \\ C_2 &= -\frac{(\mathrm{i}\omega^* + d_1\mu_{n_0} + ru^*)b + rau^*v^*}{abu^* + ru^*(\mathrm{i}\omega^* + d_2\mu_{n_0} + au^* + c)}, \\ C_3 &= \frac{(-\mathrm{i}\omega^* + d_1\mu_{n_0} + ru^*)(-\mathrm{i}\omega^* + d_2\mu_{n_0} + au^* + c) - a^2u^*v^*}{av^*\mathrm{e}^{-\mathrm{i}\omega^*\tau^*}(-\mathrm{i}\omega^* + d_2\mu_{n_0} + c)}, \\ C_4 &= \frac{(-\mathrm{i}\omega^* + d_1\mu_{n_0} + ru^*)u^* - au^*v^*}{v^*(-\mathrm{i}\omega^* + d_2\mu_{n_0} + c)} \end{aligned}$$

and

$$\overline{M} = \frac{1}{1 + C_1\overline{C_3} + C_2\overline{C_4} + \tau^*a\overline{C_3}(v^* + u^*C_2)\mathrm{e}^{-\mathrm{i}\omega\tau^*}}.$$

Obviously, $(q^*, q)_c = 1$. Then, we decompose $\mathscr{C}$ by

$$\Lambda = \{\pm i\omega^*\tau^*\},$$

$\mathscr{C} = P \oplus Q$, where

$$\begin{aligned} P &= \{zq\gamma_{n_0} + \overline{zq}\gamma_{n_0} | z \in \mathbb{C}\}, \\ Q &= \{\phi \in \mathscr{C} | (q^*\gamma_{n_0}, \phi) = 0 \text{ and } (\overline{q}^*\gamma_{n_0}, \phi) = 0\}. \end{aligned}$$

Thus, system (23) could be rewritten as

$$U_t = z(t)q(\cdot)\gamma_{n_0} + \bar{z}(t)\bar{q}(\cdot)\gamma_{n_0} + W(t, \cdot),$$

where

$$W(t, \cdot) \in Q.$$

As in Hassard et al. (1981), we have

$$z(t) = (q^* \gamma_{n_0}, U_t), \qquad W(t,\theta) = U_t(\theta) - 2\mathrm{Re}\{z(t) q(\theta) \gamma_{n_0}\}. \tag{25}$$

Then, it follows that

$$\dot{z}(t) = i\omega_0 z(t) + \bar{q}^{*\mathrm{T}}(0)\langle F(0, U_t), \beta_{n_0}\rangle, \tag{26}$$

where

$$\langle F, \beta_n\rangle := (\langle F_1, \gamma_n\rangle, \langle F_2, \gamma_n\rangle, \langle F_3, \gamma_n\rangle)^{\mathrm{T}},$$

With the center manifold theorem (Lin et al. 1992), there exists a center manifold $\mathcal{C}_0$ and on $\mathcal{C}_0$, we have

$$W(t,\theta) = W(z(t), \bar{z}(t), \theta) = W_{20}(\theta)\frac{z^2}{2} + W_{11}(\theta) z\bar{z} + W_{02}(\theta)\frac{\bar{z}^2}{2} + \cdots, \tag{27}$$

where z and $\bar{z}$ are local coordinates for center manifold $\mathcal{C}_0$ in the direction of $q\gamma_{n_0}$ and $\bar{q}\gamma_{n_0}$, respectively. For solution $U_t \in \mathcal{C}_0$, we denote

$$F(0, U_t)\ |_{\mathcal{C}_0} = \tilde{F}(0, z, \bar{z}),$$

and

$$\tilde{F}(0, z, \bar{z}) = \tilde{F}''_{zz}\frac{z^2}{2} + \tilde{F}''_{z\bar{z}} z\bar{z} + \tilde{F}''_{\bar{z}\bar{z}}\frac{\bar{z}^2}{2} + \tilde{F}''_{zz\bar{z}}\frac{z^2\bar{z}}{2} + \cdots.$$

For convenience, we rewrite (26) as

$$\dot{z}(t) = i\omega_0 z(t) + g(z, \bar{z}),$$

and denote

$$g(z, \bar{z}) = g_{20}\frac{z^2}{2} + g_{11} z\bar{z} + g_{02}\frac{\bar{z}^2}{2} + g_{21}\frac{z^2\bar{z}}{2} + \cdots.$$

From direct calculation, we get

$$\begin{aligned}
g_{20} &= 2\overline{M}\tau^* \int_\Omega \gamma_{n_0}^3 \mathrm{d}x(-r - rC_1 - aC_2 + aC_2 \mathrm{e}^{-2\mathrm{i}\omega^*\tau^*}\overline{C_3} - aC_2\overline{C_4}),\\
g_{11} &= \overline{M}\tau^* \int_\Omega \gamma_{n_0}^3 \mathrm{d}x[-2r - r(C_1 + \overline{C_1}) - a(C_2 + \overline{C_2})\\
&\quad + a(C_2 + \overline{C_2})\overline{C_3} - a(C_2 + \overline{C_2})\overline{C_4}],\\
g_{02} &= 2\overline{M}\tau^* \int_\Omega \gamma_{n_0}^3 \mathrm{d}x(-r - r\overline{C}_1 - a\overline{C}_2 + a\overline{C}_2 \mathrm{e}^{2\mathrm{i}\omega^*\tau^*}\overline{C_3} - a\overline{C}_2\overline{C_4})
\end{aligned}$$

and

$$
\begin{aligned}
g_{21} = \overline{M}\tau^* \int_\Omega \Big\{ \Big[& -r(2w_{20}^{(1)}(0) + 4w_{11}^{(1)}(0)) \\
& - r(w_{20}^{(2)}(0) + 2w_{11}^{(2)}(0) + \overline{C}_1 w_{20}^{(1)}(0) + 2C_1 w_{11}^{(1)}(0)) \\
& - a(w_{20}^{(3)}(0) + 2w_{11}^{(3)}(0) + \overline{C}_2 w_{20}^{(1)}(0) + 2C_2 w_{11}^{(1)}(0)) \Big] \gamma_{n_0}^2 \\
& + a(w_{20}^{(3)}(-1)\mathrm{e}^{\mathrm{i}\omega^*\tau^*} + 2w_{11}^{(3)}(-1)\mathrm{e}^{-\mathrm{i}\omega^*\tau^*} + \overline{C}_2 w_{20}^{(1)}(-1)\mathrm{e}^{\mathrm{i}\omega^*\tau^*} \\
& + 2C_2 w_{11}^{(1)}(-1)\mathrm{e}^{-\mathrm{i}\omega^*\tau^*})\gamma_{n_0}^2 \overline{C_3} - a(w_{20}^{(3)}(0) + 2w_{11}^{(3)}(0) \\
& + \overline{C}_2 w_{20}^{(1)}(0) + 2C_2 w_{11}^{(1)}(0))\gamma_{n_0}^2 \overline{C_4} \Big\} \mathrm{d}x.
\end{aligned}
$$

Here, w_{11} and w_{20} are need to be computed. From (25), we have

$$
\begin{aligned}
\dot{W} &= \dot{U}_t - \dot{z}q\gamma_{n_0} - \dot{\bar{z}}\bar{q}\gamma_{n_0} \\
&= \begin{cases} AW - 2\mathrm{Re}\{g(z,\bar{z})q(\theta)\}\gamma_{n_0}, & \theta \in [-r, 0), \\ AW - 2\mathrm{Re}\{g(z,\bar{z})q(\theta)\}\gamma_{n_0} + \tilde{F}, & \theta = 0, \end{cases} \\
&\doteq AW + H(z, \bar{z}, \theta),
\end{aligned} \tag{28}
$$

where

$$
H(z, \bar{z}, \theta) = H_{20}(\theta)\frac{z^2}{2} + H_{11}(\theta)z\bar{z} + H_{02}(\theta)\frac{\bar{z}^2}{2} + \cdots.
$$

Obviously,

$$
\begin{aligned}
H_{20}(\theta) &= \begin{cases} -g_{20}q(\theta)\gamma_{n_0} - \bar{g}_{02}\bar{q}(\theta)\gamma_{n_0}, & \theta \in [-r, 0), \\ -g_{20}q(0)\gamma_{n_0} - \bar{g}_{02}\bar{q}(0)\gamma_{n_0} + \tilde{F}''_{zz}, & \theta = 0, \end{cases} \\
H_{11}(\theta) &= \begin{cases} -g_{11}q(\theta)\gamma_{n_0} - \bar{g}_{11}\bar{q}(\theta)\gamma_{n_0}, & \theta \in [-r, 0), \\ -g_{11}q(0)\gamma_{n_0} - \bar{g}_{11}\bar{q}(0)\gamma_{n_0} + \tilde{F}''_{z\bar{z}}, & \theta = 0, \end{cases} \\
&\cdots.
\end{aligned}
$$

Comparing the coefficients of (28) with the derived function of (27), we obtain

$$
(A_0 - 2\mathrm{i}\omega_0 I)W_{20}(\theta) = -H_{20}(\theta), \quad A_0 W_{11}(\theta) = -H_{11}(\theta), \ \cdots. \tag{29}
$$

From (22) and (29), for $\theta \in [-1, 0)$, we have

$$
\begin{aligned}
W_{20}(\theta) &= -\frac{g_{20}}{\mathrm{i}\omega^*\tau^*}q(\theta)\gamma_{n_0} - \frac{\bar{g}_{02}}{3\mathrm{i}\omega^*\tau^*}\overline{q}(\theta)\gamma_{n_0} + E_1\mathrm{e}^{2\mathrm{i}\omega^*\tau^*\theta}, \\
W_{11}(\theta) &= \frac{g_{11}}{\mathrm{i}\omega^*\tau^*}q(0)\mathrm{e}^{\mathrm{i}\omega^*\tau^*\theta}\gamma_{n_0} - \frac{\bar{g}_{11}}{\mathrm{i}\omega^*\tau^*}\overline{q}(0)\mathrm{e}^{-\mathrm{i}\omega^*\tau^*\theta}\gamma_{n_0} + E_2,
\end{aligned} \tag{30}
$$

where E_1 and E_2 are both three-dimensional vectors in X and can be determined by setting $\theta = 0$ in H. In fact, set $\theta = 0$ and by (29) and (30), we obtain

$$(A_0 - 2\mathrm{i}\omega^*\tau^* I)E_1 \mathrm{e}^{2\mathrm{i}\omega^*\tau^*\theta} \mid_{\theta=0} = -\tilde{F}''_{zz}, \quad A_0 E_2 \mid_{\theta=0} = -\tilde{F}''_{z\bar{z}}. \tag{31}$$

The terms $\tilde{F}''_{zz}$ and $\tilde{F}''_{z\bar{z}}$ are elements in the space $\mathscr{C}$, and

$$\tilde{F}''_{zz} = \sum_{n=1}^{\infty} \langle \tilde{F}''_{zz}, \beta_n \rangle \gamma_n, \quad \tilde{F}''_{z\bar{z}} = \sum_{n=1}^{\infty} \langle \tilde{F}''_{z\bar{z}}, \beta_n \rangle \gamma_n.$$

We denote

$$E_1 = \sum_{n=0}^{\infty} E_1^n \gamma_n, \quad E_2 = \sum_{n=0}^{\infty} E_2^n \gamma_n,$$

then from (31) we have

$$\begin{aligned} &(A_0 - 2\mathrm{i}\omega^*\tau^* I)E_1^n \gamma_n \mathrm{e}^{2\mathrm{i}\omega^*\tau^*\theta} \mid_{\theta=0} = -\langle \tilde{F}''_{zz}, \beta_n \rangle \gamma_n, \\ &A_0 E_2^n \gamma_n \mid_{\theta=0} = -\langle \tilde{F}''_{z\bar{z}}, \beta_n \rangle \gamma_n, \\ &n = 0, 1, \cdots. \end{aligned}$$

Thus, E_1^n and E_2^n could be calculated by

$$\begin{aligned} E_1^n &= \left(2\mathrm{i}\omega^*\tau^* I - \int_{-1}^{0} \mathrm{e}^{2\mathrm{i}\omega^*\tau^*\theta} \mathrm{d}\eta_n(0,\theta)\right)^{-1} \langle \tilde{F}''_{zz}, \beta_n \rangle, \\ E_2^n &= -\left(\int_{-1}^{0} \mathrm{d}\eta_n(0,\theta)\right)^{-1} \langle \tilde{F}''_{z\bar{z}}, \beta_n \rangle, \\ n &= 0, 1, \cdots, \end{aligned}$$

where

$$\begin{aligned} \tilde{F}_{20} &= 2\tau^* \begin{pmatrix} -r - rC_1 - aC_2 \\ aC_2 \mathrm{e}^{-2\mathrm{i}\omega^*\tau^*} \\ -aC_2 \end{pmatrix}, \\ \tilde{F}_{11} &= \tau^* \begin{pmatrix} -2r - r(C_1 + \overline{C}_1) - a(C_2 + \overline{C}_2) \\ a(C_2 + \overline{C}_2) \\ -a(C_2 + \overline{C}_2) \end{pmatrix}. \end{aligned}$$

Hence, g_{21} could be represented explicitly.

We denote

$$c_1(0) = \frac{i}{2\omega^*\tau^*}\left(g_{20}g_{11} - 2|g_{11}|^2 - \frac{1}{3}|g_{02}|^2\right) + \frac{1}{2}g_{21},$$

$$\mu = -\frac{\mathrm{Re}(c_1(0))}{\tau^*\mathrm{Re}(\lambda'(\tau^*))}, \quad \beta_2 = 2\mathrm{Re}(c_1(0)),$$
$$T_2 = -\frac{1}{\omega^*\tau^*}(\mathrm{Im}(c_1(0)) + \mu_2(\omega^* + \tau^*\mathrm{Im}(\lambda'(\tau^*)))). \tag{32}$$

Then, by the general Hopf bifurcation theory (see Hassard et al. 1981), we know that μ determines the directions of the Hopf bifurcation: If $\mu > 0 (< 0)$, then the direction of the Hopf bifurcation is forward (backward), that is the bifurcating periodic solutions exist when $a > 0 (< 0)$; β_2 determines the stability of the bifurcating periodic solutions: The bifurcating periodic solutions are orbitally stable(unstable) if $\beta_2 < 0 (> 0)$, and T_2 determines the period of the bifurcation periodic solutions: The period increases(decreases) if $T_2 > 0 (< 0)$.

We now describe briefly the numerical method we use to solve the system (5) as follows. For $\Omega = (0, p\pi) \times (0, q\pi)$, let $x_i = ih_x, i = 1, 2, \cdots, l, h_x = \frac{p\pi}{l}$, $y_j = jh_y, j = 1, 2, \cdots, m, h_y = \frac{q\pi}{m}$, , $t_k = kh_t, h_t = \frac{\tau}{N}$ (N is a positive integer), and $u(i, j, k) = u(x_i, y_j, t_k)$, $v(i, j, k) = v(x_i, y_j, t_k)$, $w(i, j, k) = w(x_i, y_j, t_k)$. We replace $\frac{\partial u(x_i, y_j, t_k)}{\partial t}$ with a first-order difference $\frac{u(i,j,k+1)-u(i,j,k)}{h_t}$ and replace $\frac{\partial^2 u(x_i, y_j, t_k)}{\partial x^2} + \frac{\partial^2 u(x_i, y_j, t_k)}{\partial y^2}$ with a second-order difference $\frac{u(i+1,j,k)-2u(i,j,k)+u(i-1,j,k)}{h_x} + \frac{u(i,j+1,k)-2u(i,j,k)+u(i,j-1,k)}{h_y}$. Similarly, we take differences of the partial derivative of v and w. Then, we get a system of difference equations:

$$\begin{cases} u(i, j, k+1) = u(i, j, k) + h_t d_1 \left(\frac{u(i+1,j,k)-2u(i,j,k)+u(i-1,j,k)}{h_x} \right. \\ \qquad \left. + \frac{u(i,j+1,k)-2u(i,j,k)+u(i,j-1,k)}{h_y} \right) \\ \qquad + h_t(ru(i, j, k)(1 - u(i, j, k) - w(i, j, k)) - au(i, j, k)v(i, j, k)), \\ w(i, j, k+1) = w(i, j, k) + h_t d_1 \left(\frac{w(i+1,j,k)-2w(i,j,k)+w(i-1,j,k)}{h_x} \right. \\ \qquad \left. + \frac{w(i,j+1,k)-2w(i,j,k)+w(i,j-1,k)}{h_y} \right) \\ \qquad + h_t(au(i, j, k - N)v(i, j, k - N) - w(i, j, k)), \\ v(i, j, k+1) = v(i, j, k) + h_t d_2 \left(\frac{v(i+1,j,k)-2v(i,j,k)+v(i-1,j,k)}{h_x} \right. \\ \qquad \left. + \frac{v(i,j+1,k)-2v(i,j,k)+v(i,j-1,k)}{h_y} \right) \\ \qquad + h_t(bw(i, j, k) - au(i, j, k)v(i, j, k) - cv(i, j, k)). \end{cases}$$

We implement this method in MATLAB and obtain numerical solutions of the system (5).

References

Bajzer Ž, Carr T, Josić K et al (2008) Modeling of cancer virotherapy with recombinant measles viruses. J Theor Biol 252(1):109–122

Barish S, Ochs MF, Sontag EO, Gevertz J (2017) Evaluation optimal therapy robustness by virtual expansion of a sample population, with a case study in cancer immunotherapy. In: PNAS E6277–E6286

Boeuf FL, Batenchuk C, Koskela MV, Breton S, Roy D, Lemay C et al (1974) Model-based rational design of an oncolytic virus with improved therapeutic potential. Nat Commun 2013:4

Chiocca EA (2002) Oncolytic viruses. Nat Rev Cancer 2(12):938

Chiocca EA, Rabkin SD (2014) Oncolytic viruses and their application to cancer immunotherapy. Cancer Immunol Res 2(4):295–300
Choudhury B, Nasipuri B (2014) Efficient virotherapy of cancer in the presence of immune response. Int J Dyn Control 2:314–325
Faria T (2000) Normal forms and Hopf bifurcation for partial differential equations with delays. Trans Am Math Soc 352(5):2217–2238
Friedman A, Lai X (2018) Combination therapy for cancer with oncolytic virus and checkpoint inhibitor: a mathematical model. PloS ONE 13(2):e0192449
Friedman A, Tian JP, Fulci G et al (2006) Glioma virotherapy: effects of innate immune suppression and increased viral replication capacity. Cancer Res 66(4):2314–2319
Harpold HL, Alvord EC Jr, Swanson KR (2007) The evolution of mathematical modeling of glioma proliferation and invasion. J Neuropathol Exp Neurol 66(1):1–9
Hassard BD, Kazarinoff ND, Wan YH (1981) Theory and applications of Hopf bifurcation. Cambridge University Press, Cambridge
Jenner AL, Coster ACF, Kim PS, Frascoli F (2018) Treating cancerous cells with viruses: insights from a minimal model for oncolytic virotherapy. Lett Biomath 5:S117–S136. https://doi.org/10.1080/23737867.2018.1440977
Kaplan JM (2005) Adenovirus-based cancer gene therapy. Curr Gene Ther 5(6):595–605
Karev GP, Novozhilov AS, Koonin EV (2006) Mathematical modeling of tumor therapy with oncolytic viruses: effects of parametric heterogeneity on cell dynamics. Biol Direct 1(1):30
Kirn DH, McCormick F (1996) Replicating viruses as selective cancer therapeutics. Mol Med Today 2(12):519–527
Lawler SE, Speranza MC, Cho CF et al (2017) Oncolytic viruses in cancer treatment: a review. JAMA Oncol 3(6):841–849
Lin X, So JWH, Wu J (1992) Centre manifolds for partial differential equations with delays. Proc R Soc Edinb Sect A Math 122(3–4):237–254
Mahasa KJ, Eladdadi A, Pillis L d, Ouifki R (2017) Oncolytic potency and reduced vuris tumor-specificity in oncolytic virotherapy, a mathematical modeling approach. PloS ONE 12(9):e0184347
Maroun J, Muñoz-Alía M, Ammayappan A, Schulze A, Peng KW, Russell S (2017) Designing and building oncolytic viruses. Future Virol 12(4):193–213
Martuza RL, Malick A, Markert JM et al (1991) Experimental therapy of human glioma by means of a genetically engineered virus mutant. Science 252(5007):854–856
Massey SC, Rockne RC, Hawkins-Daarud A, Gallaher J, Anderson ARA, Canoll P, Swanson KR (2018) Simulating PDGF-driven glioma growth and invasion in an anatomically accurate brain domain. Bull Math Biol 80:1292–12309
Mok W, Stylianopoulos T, Boucher Y, Jain RK (2009) Mathematical modeling of herpes simplex virus distribution in solid tumors: implications for cancer gene therapy. Clin Cancer Res 15(7):2352–2360
Novozhilov AS, Berezovskaya FS, Koonin EV et al (2006) Mathematical modeling of tumor therapy with oncolytic viruses: regimes with complete tumor elimination within the framework of deterministic models. Biol Direct 1(1):6
Phan TA, Tian JP (2017) The role of the innate immune system in oncolytic virotherapy. Comput Math Methods Med 6587258
Ratajczyk E, Ledzewicz U, Leszczynski M, Schattler H (2018) Treatment of glioma with virotherapy and TNF-a inhibitors: analysis as a dynamical system. Discrete Contin Dyn Syst B 23(1):425–441
Roberts MS, Lorence RM, Groene WS et al (2006) Naturally oncolytic viruses. Curr Opin Mol Ther 8(4):314–321
Swanson KR, Alvord EC, Murray JD (2002) Virtual brain tumours (gliomas) enhance the reality of medical imaging and highlight inadequacies of current therapy. Br J Cancer 86:14–18
Tian JP (2011) The replicability of oncolytic virus: defining conditions in tumor virotherapy. Math Biosci Eng 8(3):841–860
Timalsina A, Tian JP, Wang J (2017) Mathematical and computational modeling for tumor virotherapy with mediated immunity. Bull Math Biol 79(8):1736–1758
Vasiliu D, Tian JP (2011) Periodic solutions of a model for tumor virotherapy. Discrete Contin Dyn Syst S 4(6):1587–1597
Wang Y, Tian JP, Wei J (2013) Lytic cycle: a defining process in oncolytic virotherapy. Appl Math Model 37(8):5962–5978

Wang Z, Guo Z, Peng H (2017) Dynamical behavior of a new oncolytic virotherapy model based on gene variation. Discrete Contin Dyn Syst S 10(5):1079–1093
Wares J, Crivelli J, Yun CO, Choi IK, Gevertz J, Kim P (2015) Treatment strategies for combining immunostimulatory oncolytic virus therapeutics with dendritic cell injections. Math Biosci Eng 2(6):1237–1256
Wein LM, Wu JT, Kirn DH (2003) Validation and analysis of a mathematical model of a replication-competent oncolytic virus for cancer treatment: implications for virus design and delivery. Cancer Res 63(6):1317–1324
Wodarz D (2001) Viruses as antitumor weapons: defining conditions for tumor remission. Cancer Res 61(8):3501–3507
Wodarz D, Komarova N (2009) Towards predictive computational models of oncolytic virus therapy: basis for experimental validation and model selection. PloS ONE 4(1):e4271
Wodarz D, Hofacre A, Lau JW, Sun Z, Fan H, Komarova N (2012) Complex spatial dynamics of oncolytic viruses in vitro: mathematical and experimental approaches. PloS Comput Biol 8(6):e1002547
Wu J (2012) Theory and applications of partial functional differential equations. Springer, Berlin
Wu JT, Byrne HM, Kirn DH et al (2001) Modeling and analysis of a virus that replicates selectively in tumor cells. Bull Math Biol 63(4):731